Environmental Research Letters

LETTER • OPEN ACCESS

Mid-21st century ozone air quality and health burden in China under emissions scenarios and climate change

View the article online for updates and enhancements.

Environmental Research Letters

LETTER

Mid-21st century ozone air quality and health burden in China under emissions scenarios and climate change

D M Westervelt[1,2] , C T Ma[3], M Z He[4], A M Fiore[1,5], P L Kinney[6], M-A Kioumourtzoglou[4], S Wang[7], J Xing[7], D Ding[7] and G Correa[1]

[1] Lamont-Doherty Earth Observatory, Columbia University. Palisades, New York, United States of America
[2] NASA Goddard Institute for Space Studies, New York, New York, United States of America
[3] Yale University, Department of Geology and Geophysics, New Haven, Connecticut, United States of America
[4] Department of Environmental Health Sciences, Columbia University Mailman School of Public Health, New York, New York, United States of America
[5] Department of Earth and Environmental Sciences, Columbia University, Palisades, New York, United States of America
[6] School of Public Health, Boston University, Boston, Massachusetts, United States of America
[7] School of Environment, Tsinghua University, Beijing, People's Republic of China

E-mail: danielmw@ldeo.columbia.edu

Keywords: ozone, climate change, China, health, model

Supplementary material for this article is available online

Abstract

Despite modest emissions reductions of air pollutants in recent years, China still suffers from poor air quality, and the outlook for future air quality in China is uncertain. We explore the impact of two disparate 2050 emissions scenarios relative to 2015 in the context of a changing climate with the Geophysical Fluid Dynamics Laboratory Atmospheric Model version 3 (GFDL-AM3) chemistry-climate model. We impose the same near-term climate change for both emission scenarios by setting global sea surface temperature (SST) and sea ice cover (SIC) to the average over 2010–2019 and 2046–2055, respectively, from a three-member ensemble of GFDL coupled climate model simulations under the RCP8.5 (Representative Concentration Pathway) scenario. By the 2050s, annual mean surface ozone increases throughout China by up to 8 ppbv from climate change alone (estimated by holding air pollutants at 2015 levels while setting SIC and SST to 2050 conditions in the model) and by 8–12 ppbv in a scenario in which emissions of ozone precursors nitrogen oxides (NO_x) and anthropogenic volatile organic compounds (VOCs) increase by ∼10%. In a scenario in which NO_x and anthropogenic VOC emissions decline by 60%, annual mean surface ozone over China decreases by 16–20 ppbv in the 2050s relative to the 2010s. The ozone increase from climate change alone results in an additional 62 000 premature deaths in China as compared to 330 000 fewer premature deaths by the 2050s under a strong emissions mitigation scenario. In springtime over Southwestern China in the 2050s, the model projects 9–12 ppbv enhancements to surface ozone from the stratosphere (diagnosed with a model tracer) and from international anthropogenic emissions (diagnosed by differencing AM3 simulations with the same emissions within China but higher versus lower emissions in the rest of the world). Our findings highlight the effectiveness of emissions controls in reducing the health burden in China due to air pollution, and also the potential for climate change and rising global emissions to offset, at least partially, some of the ozone decreases attained with regional emission reductions in China.

1. Introduction

Exposure to surface ozone causes hundreds of thousands of premature deaths worldwide each year (Cohen *et al* 2017), and is associated with morbidity, damage to ecosystems and crops, and in the upper troposphere is an important greenhouse gas (Myhre *et al* 2013, Jhun *et al* 2014, Tai *et al* 2014, Yue and

Unger 2014). In China, 67 000 premature deaths were attributed to ozone in 2015, among the largest premature mortality from ozone air pollution in the world (Cohen *et al* 2017). Some tropospheric ozone originates in the stratosphere, which occasionally may enhance concentrations at the surface and impact air quality in some regions and seasons (Langford *et al* 2009, Lin *et al* 2012). In addition to emissions, climate change influences ozone air quality through changes in temperature, atmospheric circulation, precipitation, and dry deposition (Jacob and Winner 2009, Fiore *et al* 2015). Though there is now evidence that emissions of ozone precursors have declined slightly in recent years in certain parts of China (Liu *et al* 2017), the future of ozone air quality in China remains uncertain and depends strongly on future emissions policies and climate change. Recent evidence points to an increase in ozone concentrations associated with particulate matter decreases in recent years in China due to the weakening of the aerosol sink of peroxy radicals (Li *et al* 2018), implying a growing need for considering future ozone air quality over China.

Over China specifically, Chen *et al* (2018) projected a 1–10 ppbv increase in annual mean ozone by 2055 (compared to 2015) using the RCP8.5 scenario in the GFDL-CM3 climate model and a statistical downscaling technique based on observed ozone distributions. Zhu and Liao (2016) used a nested version of the global chemical transport model GEOS-Chem with the RCP emissions scenarios and found increases in annual mean surface ozone of 6–12 ppbv by 2050 (relative to 2000) in the RCP6.0 and RCP8.5 scenario, and decreases of up to 6 ppbv in RCP2.6 and RCP4.5. Wang *et al* (2013) also used GEOS-Chem but with the SRES A1B scenario, finding summertime increase in mean surface ozone of 0.4 ppbv due to climate change alone, and an increase of 11.6 ppbv due to emissions changes alone over the period 2000–2050. Liu *et al* (2013) found autumn season increases in surface ozone of up to 6.1 ppbv from emissions alone and 1.5 ppbv from climate change in the Pearl River Delta region of China, using the Weather Research and Forecasting with Chemistry model (WRF-Chem) and the SRES A1B future emissions scenario. Fiore *et al* (2012) synthesized several multimodel studies using a variety of future emissions projections on emissions and climate-driven changes to future ozone, and found a wide range (±4 ppbv) for climate-driven ozone and emissions-driven ozone (−4 to +10 ppbv) over East Asia, though their domain included Korea and Japan. Models are in qualitative agreement on future climate-driven ozone over China, but the sign and magnitude of change vary strongly with the selected emissions scenario.

Here, we use a more recent emissions inventory, ECLIPSE v5a (Evaluating the Climate and Air Quality Impacts of Short-Lived Pollutants) CLE (Current Legislation) and Maximum technically Feasible Reduction (MFR) scenarios for estimates of future emissions globally and over China (Stohl *et al* 2015). These future emissions projections include substantial improvements over previous emissions scenarios, especially over China, where large changes have recently occurred. ECLIPSE takes into account new emissions control policies announced under China's 12th five-year plan that were not previously considered in other inventories. It also considers a number of newer emissions standards released after 2010 and includes integrated policies that include both energy-saving measures and end-of-pipe controls (Wang *et al* 2014). ECLIPSE also represents a wider range of possible emissions futures for China and the rest of the world, which is an improvement over the SRES and RCP scenarios. Kirtman *et al* (2013) compared air pollutant emissions projections under SRES and RCPs, finding that the RCP emissions were smaller than SRES by a factor of 1.2–3.

We focus on the impact of climate change and emissions scenarios on surface ozone over China (section 3), using GFDL-AM3, described and evaluated in section 2 and supplementary information (available online at stacks.iop.org/ERL/14/074030/mmedia). We examine the impact of stratospheric-tropospheric transport and the sensitivity of surface ozone to temperature on future ozone levels in China (section 3). Finally, using methodology from a recent long term study of ozone mortality (Turner *et al* 2016), we calculate the human health burden in China associated with future ozone exposure projections (section 4).

2. Methods

We use the atmospheric component of the NOAA GFDL AM3 (Donner *et al* 2011) to perform simulations of present and future climate under different emissions scenarios provided by the ECLIPSE v5a inventory. ECLIPSE provides present-day (2015) emissions of SO_2, NO_x, NH_3, NMVOC, BC, OC, $PM_{2.5}$, PM_{10}, and CO, and future emissions in the current legislation (CLE) and MFR (Stohl *et al* 2015). CLE and MFR are described in further detail in the supplement. We simulate a base-case for comparison with future scenarios, with year 2015 emissions (where MFR and CLE emissions are identical) and 2015 climate. All simulations, both present-day base case and future projections for 2050 are 10 years in length and repeat 2015 (or 2050) climate and emissions continuously for those 10 years. Climatic conditions are specified using global sea surface temperatures (SST) and sea ice cover (SIC) according to decadal averages for the years 2010–2019 for present day and 2046–2055 for the future from a three-member ensemble of GFDL-CM3 transient simulations under the RCP8.5 high warming scenario. The decadal averages of the combined three-member ensembles help dampen climate variability arising from the ocean (but atmospheric variability remains).

Table 1. Simulation name, emissions scenarios (CLE/MFR and year of emissions), climate change scenario (year of SST and SIC input from RCP8.5 three-member ensemble simulations of GFDL-CM3), and emissions of NO_x, NMVOC, and CO over China and globally. Units for NO_x: Tg NO_2 yr^{-1}; units for NMVOC: Tg NMVOC yr^{-1}; units for CO: Tg CO yr^{-1}.

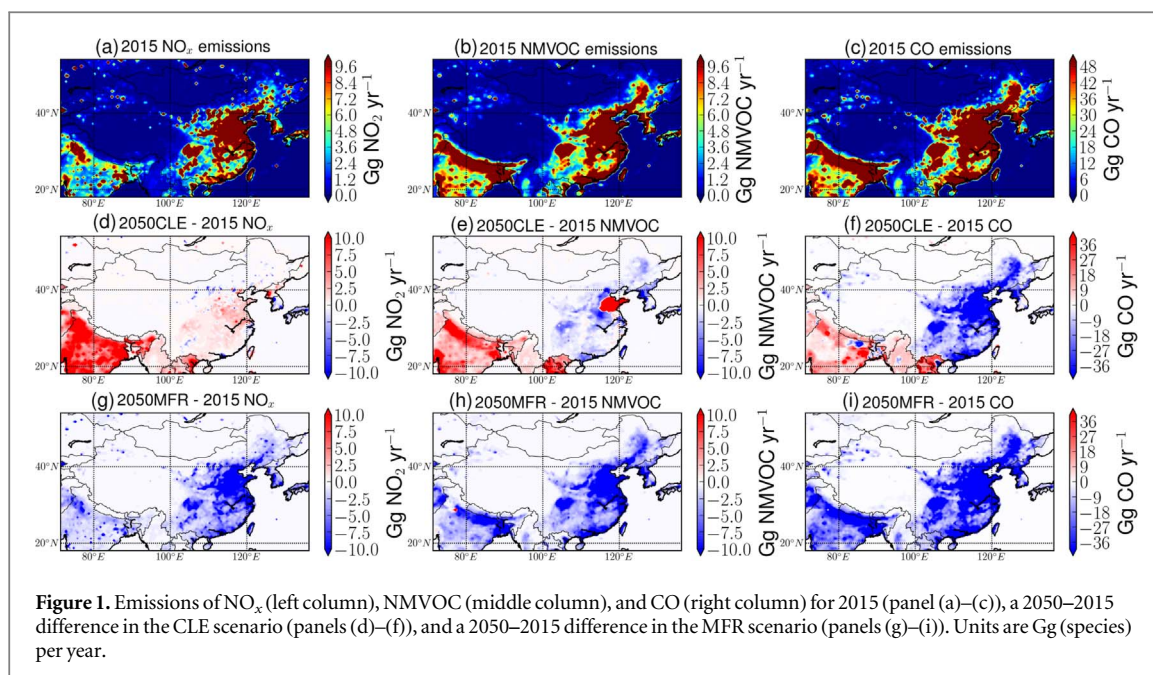| Name	Emission scenario	China emissions			Global emissions			Climate change scenario
		NO_x	NMVOC	CO	NO_x	NMVOC	CO	
2015	CLE 2015	20.6	24.2	163	91.5	108	520	2015
2050 CLE	CLE 2050	25.1	25.5	120	112	121	501	2050
2050 MFR	MFR 2050	8.52	9.04	45.2	31.4	50.3	165	2050
2050 CLIM	CLE 2015	20.6	24.2	163	91.5	108	520	2050
2050 CHMFR	MFR over China only, CLE elsewhere	8.52	9.04	45.2	91.5	108	520	2050

The CLE and MFR scenarios do not provide concentrations of CO_2 and other long-lived greenhouse gases needed to drive climate forcing. As such, we use the long-lived greenhouse gases from the RCP8.5 scenario that are consistent with the SST and SIC in our 2015 and 2050 AM3 simulations. We impose the same SSTs, SICs, and well-mixed greenhouse gases (RCP8.5) in 2050 for both air pollution scenarios (CLE and MFR) to facilitate a more direct comparison between the roles of emission changes under the CLE versus MFR scenario. Coupling a high warming scenario such as RCP8.5 with a strong air pollution emissions mitigation scenario such as MFR is indicative of a future with aggressive end-of-pipe air pollution control technology limiting NO_x but doing little to mitigate long-lived greenhouse gases such as CO_2. Qualitatively, this RCP8.5-MFR scenario is similar to the SSP5-8.5 scenario for phase 6 of the Coupled Model Intercomparison Project (CMIP6), which combines a strong air pollution control scenario in the Shared Socioeconimc Pathway 5 (SSP5) with a high warming endpoint (8.5 W m^{-2} radiative forcing by 2100) (O'Neill *et al* 2016). In all of our simulations, methane concentrations are held at 2015 levels with respect to atmospheric chemistry, but increase according to RCP8.5 for the radiative effect by imposing different methane abundances in the chemistry versus radiative transfer modules. CO_2 and other tropospheric nonreactive greenhouse gases are also prescribed to 2050 levels. These simulations include the combined impact of climate and emissions changes.

We also simulate the impact of future climate change alone on surface ozone by holding anthropogenic emissions of aerosols and ozone precursors at 2015 levels but using a 2050 decadal mean climate. We chose to use 2015 emissions as the fixed baseline because emissions are identical between CLE and MFR for the year 2015, but are vastly different in the future. We take the difference between the present-day simulation and the future time-slice simulations to quantify the change in surface ozone. To estimate the impact of Chinese emissions reductions alone on ozone air quality beyond China (e.g. Western US), we simulate 2050 with MFR emissions over China (CHMFR in table 1)

but CLE emissions elsewhere and subtract this simulation from the simulation with CLE emissions applied globally. The difference between the CHMFR simulation and the global MFR emissions provides an estimate of how growth in global emissions outside of China could influence future air quality over China.

To quantify stratospheric ozone influence in surface air, all of our simulations use the 'O3S_e90' tracer approach to quantify stratospheric contributions to surface ozone as defined in Lin *et al* (2012). Briefly, this stratospheric ozone tagging method utilizes a tropopause tracer with a globally uniform surface source and a 90 d e-folding lifetime (Prather *et al* 2011) to define the tropopause. Stratospheric air is defined as where the e90 mixing ratio is less than 85 ppbv, and ozone in the stratosphere is tagged as 'O3S_e90'. We estimate changes in the stratospheric ozone contribution to surface air as the difference in this tracer between simulations.

The GFDL-AM3 present-day (2015) simulation is evaluated against hourly observations from 1494 monitoring stations across 364 cities in China from the period of 1 January 2015–31 December 2015 in section 4 of the supplementary information. Figure S3 shows monthly mean maximum daily 8 h average values (MDA8) across a geographically diverse set of urban locations throughout China. Although the model is biased high due to uncertainties in emissions of anthropogenic and biogenic precursors, uncertainties in ozone sinks such as dry deposition, and inability of the coarse resolution model (~200 km by 200 km) to resolve ozone titration and other chemical processes occurring at local scales, we focus our analysis on differences between model simulations of the future and present. To the extent that biases impact ozone concentrations in an equivalent manner in the present and future, our estimates of changes should be minimally affected by this mean state bias. Earlier work suggests that despite similarly high biases in the eastern US in summer, the modeled response to NO_x emissions reductions phased in from the late 1990s–2000s is captured (Clifton *et al* 2014, Rieder *et al* 2015). Therefore, to our best understanding we expect that the bias stems from simulating the mean ozone

Figure 1. Emissions of NO$_x$ (left column), NMVOC (middle column), and CO (right column) for 2015 (panel (a)–(c)), a 2050–2015 difference in the CLE scenario (panels (d)–(f)), and a 2050–2015 difference in the MFR scenario (panels (g)–(i)). Units are Gg (species) per year.

abundances rather than the sensitivity of ozone to changes in emissions or meteorology. Rieder *et al* (2015) and Chen *et al* (2018) used a quantile mapping bias correction method on GFDL-AM3 ozone, using the same correction for both present and future, assuming bias is systematic and stationary. However, since we focus on changes in ozone concentration and mortality between 2015 and 2050, applying their method would simply result in cancellation of the bias correction.

3. Projected changes in surface ozone concentrations over China in the 21st century
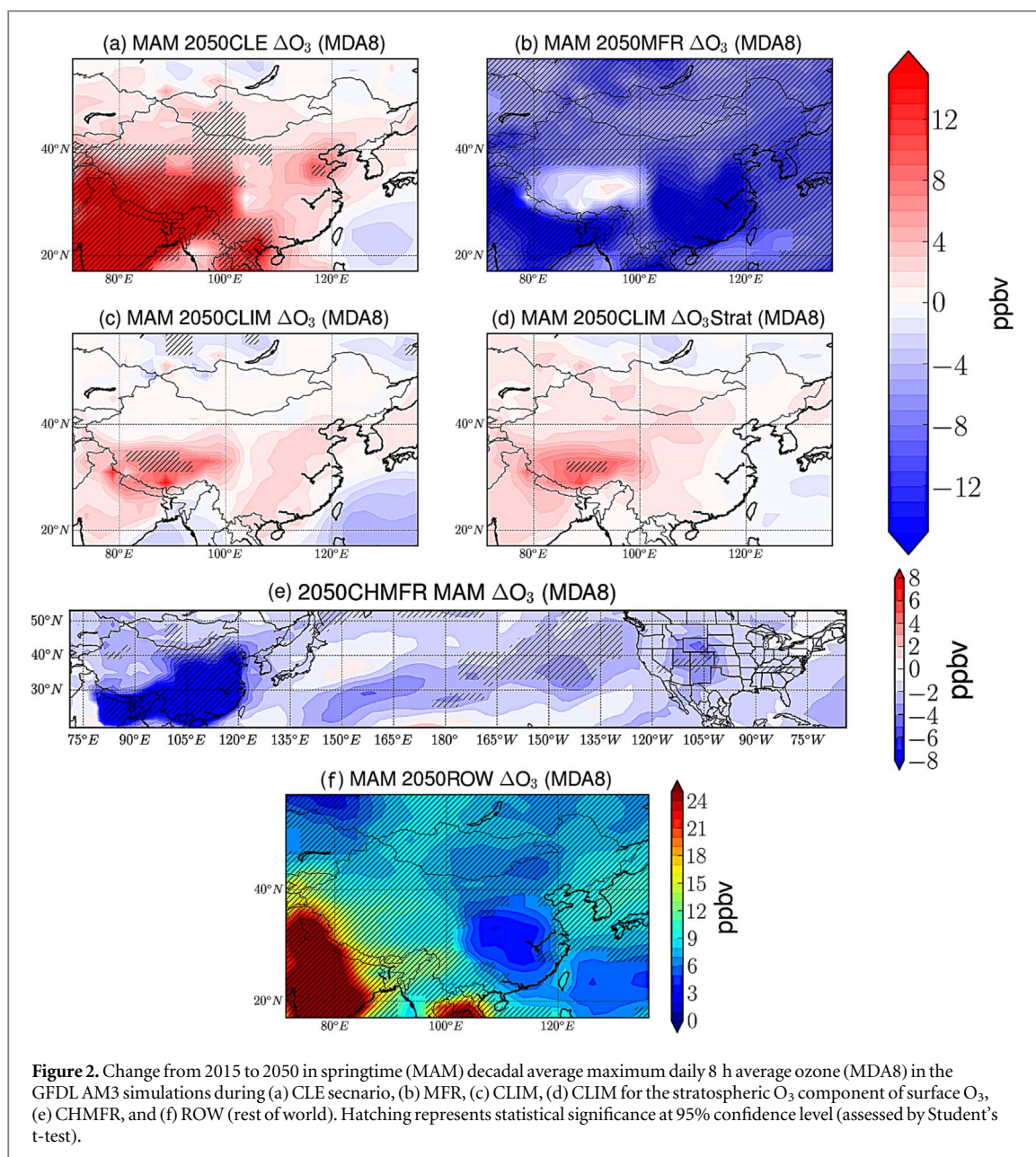
3.1. From emissions within and outside China
Figure 1 shows the spatial distribution of NMVOC, NO$_x$, and CO emissions in 2015 and the difference between 2015 and 2050 for the MFR and CLE scenarios over China. In the CLE scenario, NO$_x$ emissions are projected to stay similar to 2015 levels by 2050, with modest increases (up to about 5 Gg NO$_2$ yr^{-1} in local hotspots) in eastern China. Anthropogenic NMVOC emissions are projected to increase by upwards of 10 Gg NMVOC yr^{-1} only on the Shandong Peninsula, surrounded by decreases of similar magnitude elsewhere in eastern China. CO emissions are projected to decrease uniformly throughout China by 2050. In the MFR scenario, emissions of all three species are projected to decrease throughout China. Table 1 and figure S1 shows the total emissions for CLE and MFR totaled over eastern China (100 °E–130°E, 20 °N–50 °N), and figure S2 shows the global total emissions. In MFR, global emissions of NO$_x$, NMVOCs, and CO are more than halved by 2050. MFR can therefore be considered an

optimistic scenario in contrast with a more status-quo scenario in CLE.

During spring and summer, when ozone concentrations are generally highest across China (figures S3 and S4), decadal average seasonal mean Chinese MDA8 surface ozone increases by up to 10 ppbv, respectively, from the 2015 to 2050 CLE simulations (figure 2(a), see figure S5 for all seasons), reflecting increases in precursor NO$_x$ and VOC emissions. Increases in ozone in eastern China, especially near the Shandong peninsula, are significant at the 95% confidence level according to a Student's t-test. Changes in southern and western China are also significant, particularly in spring over the majority of western China. The ozone increase over the Tibetan Plateau region in southwestern China partially reflects the influence from the nearby Indo-Gangetic Plain, where emissions of ozone precursors are projected to increase by 50%. In contrast with CLE, statistically significant ozone decreases occur uniformly in the MFR scenario in every season (figures 2(b), S7), echoing the changes in emissions of ozone precursors in the ECLIPSE inventory (figure 1 and table 1). Ozone decreases are highest in summer (JJA, figure S6), when they reach upward of 20 ppbv over almost the entire domain, and lowest in winter (DJF, figure S6). Ozone decreases are largest in the central and southern parts of eastern China, mostly at or below the latitude of the Yellow Sea. The standard deviation of annual mean MDA8 ozone in present-day simulations is 1.7 ppbv averaged over China and less than 2 ppbv for any given season (figure S7), suggesting that the changes in future ozone in CLE and MFR and subsequent changes described below are significant compared to internal variability.

Figure 2(e) shows the change in MDA8 surface ozone due to a major reduction in ozone precursor emissions over China only by 2050 with the rest of the

Figure 2. Change from 2015 to 2050 in springtime (MAM) decadal average maximum daily 8 h average ozone (MDA8) in the GFDL AM3 simulations during (a) CLE secnario, (b) MFR, (c) CLIM, (d) CLIM for the stratospheric O_3 component of surface O_3, (e) CHMFR, and (f) ROW (rest of world). Hatching represents statistical significance at 95% confidence level (assessed by Student's t-test).

world following CLE (referred to hereafter as 2050CHMFR). The 2050CHMFR hybrid scenario is differenced against 2050CLE (higher emissions CLE scenario everywhere, including China), thus isolating the impact of Chinese emissions reductions alone. In the springtime, when observations and models indicate intercontinental transport of air pollution over the Pacific peaks (Task Force on Hemispheric of Air Pollution 2010), significant (hatching) surface ozone decreases of up to 6–8 ppbv occur in the western US. These changes are largest over higher elevations in the US (Rocky Mountains), which are more susceptible to changes in free tropospheric ozone transport. While climate variability will modulate the impact of Chinese emissions reductions on US surface ozone via intercontinental transport (which can be amplified or dampened by variability in stratosphere-troposphere transport as shown in Lin *et al* 2015), our results imply

that aggressive emission reductions over China would reduce ozone concentrations over the western US.

We further examine the implications for air quality over China in 2050 if China aggressively reduces ozone precursor emissions according to MFR but the rest of the world follows CLE instead of MFR. Here, the hybrid scenario described above is differenced against 2050MFR (instead of 2050CLE), thereby isolating the influence of the emissions difference between CLE and MFR in the rest of the world on China (called 2050ROW). Under this scenario, we find statistically significant higher surface MDA8 ozone in springtime (figure 2(f), all seasons figure S8) across most of China, largest (up to 15 ppbv) in western China in close proximity to India. Emissions of NO_x in India increase by 25% in CLE and 50% specifically in northwest India, which strongly impacts western China ozone concentrations in all seasons. In eastern

China, increases are smaller (less than 6 ppbv) due to a larger influence of local emissions. However, the influence of foreign emissions still impacts several areas in eastern China by 15 ppbv or more in the summer (figure S8). Increases in ozone of up to 9 ppbv occur in south China, which may reflect an influence of pollution from countries in Southeast Asia.

3.2. From climate change

Surface MDA8 ozone changes in the 2050CLIM simulation relative to the 2015 simulation (in which precursors of ozone and aerosols are held at 2015 levels) are shown in figure 2(c) (see figure S9 for all other seasons). Consistent with previous work, ozone increases due to future climate change in polluted regions (e.g. high emissions in figure 1). The increases are largest in the summer and fall months in Western China (up to 8 ppbv, figure S9), but occur year round, with an annual mean increase of about 4 ppbv over populous eastern China. Statistical significance is most widespread in western China especially over the Tibetan Plateau and in close proximity to India. The increases in surface ozone near major cities on the east coast of China, near the Yangtze River region, and sporadically in other areas are only significant in autumn. While climate-driven changes in surface ozone are generally smaller in magnitude than the emission-driven changes, as expected, these 4 ppbv seasonal increases in the heavily populated eastern portion of China could become more important in meeting ozone targets in the future as China aims to reduce its air pollution health burden. These climate-driven O_3 changes would likely be smaller if a future emissions scenario such as MFR in 2050 was used as the fixed baseline, since the sensitivity of O_3 to temperature decreases with decreasing regional NO_x emissions (Rasmussen *et al* 2012).

We find that the springtime increases in southwestern China reflect increasing stratospheric ozone. Figure 2(d) shows the change in the stratospheric ozone component of springtime surface MDA8 ozone (O_3S; see figure S10 for all seasons) in 2050CLIM from 2015 to 2050. The change in O_3S over the Tibetan Plateau or anywhere else in China is statistically significant at the 95% confidence level only in spring (hatching in figure 2(d)). This O_3S increase also occurs in 2050CLE and 2050MFR (figures S11 and S12), which are driven by the same 2050 SSTs and sea ice as 2050CLIM, suggesting that this enhanced stratospheric transport is a robust feature of future climate change in this model. In the spring, climate-driven stratospheric ozone contributes as much as 12 ppbv to surface ozone over the high elevation Tibetan Plateau, or 15% compared to present-day surface ozone levels in an area that is not as heavily influenced by localized anthropogenic emissions compared to populated urban centers of eastern China. The surface ozone increase in 2050 in the MFR scenario in spring

(figure 1(c)) in this region suggests that climate-driven increases in stratospheric influence on surface air are sufficient to offset the ozone reductions produced by the widespread emissions decreases in the MFR scenario (figure 1). Surface ozone increases in 2050 are also enhanced in the CLE scenario (which has the same climate forcing, but also includes air pollutant emission changes) by the stratospheric component.
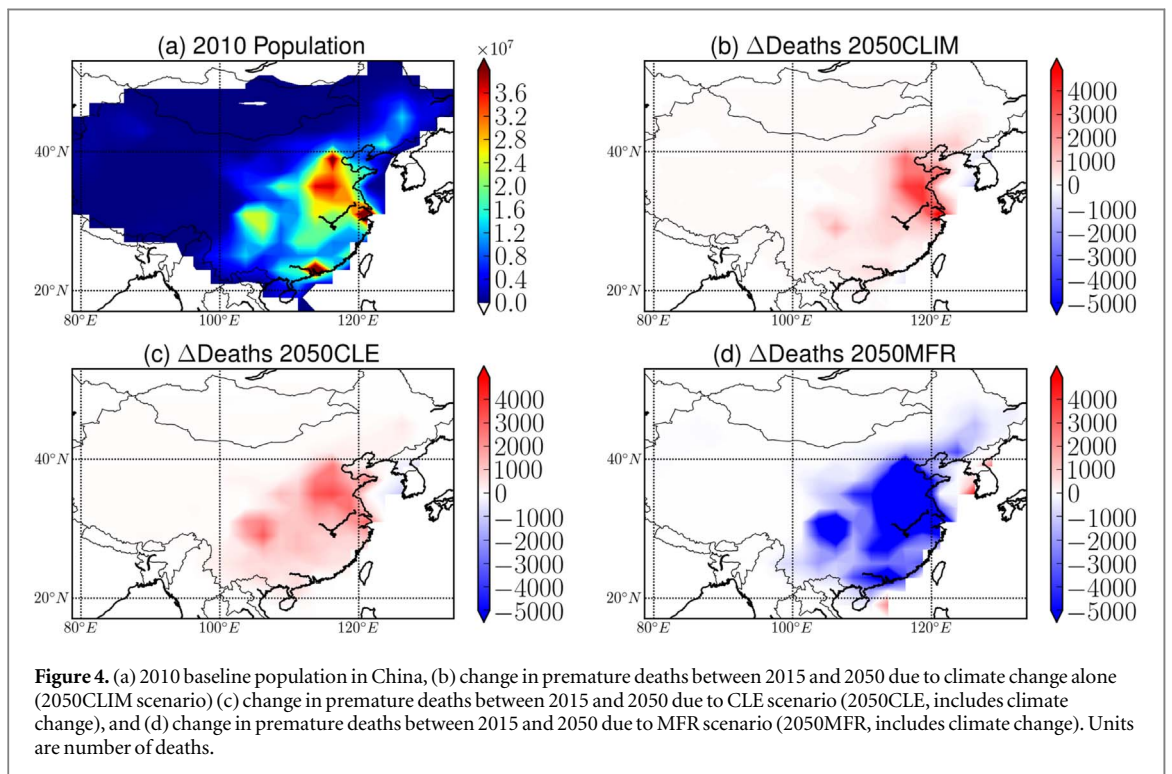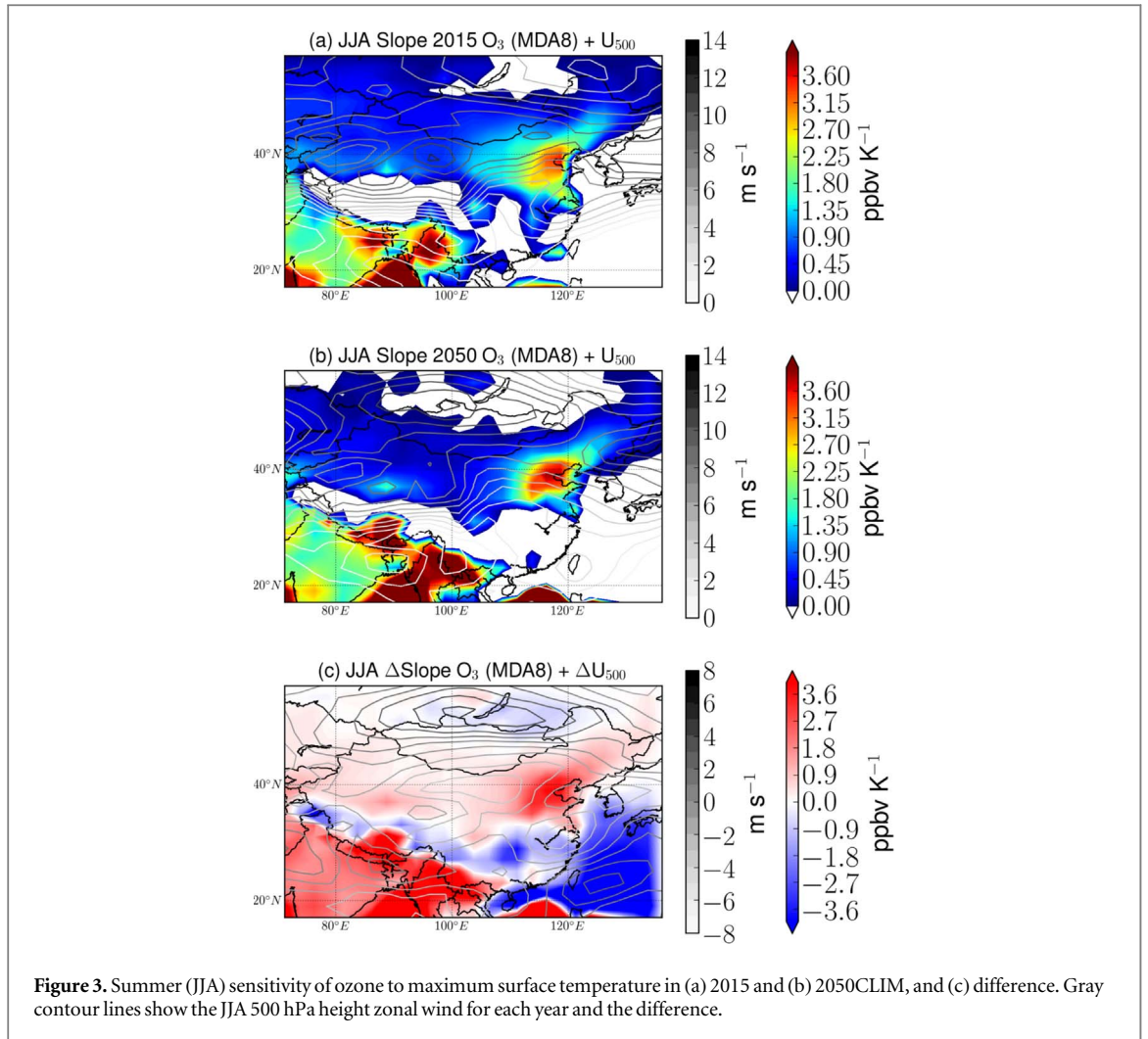
Figure 3 shows the MDA8 surface ozone versus maximum daily temperature (T_{max}) slope (ppbv K^{-1}) in summer time over China in 2015 and in 2050 in the climate change only scenario (2050CLIM). Correlations between T_{max} and MDA8 ozone are shown in figure S13. In 2015, ozone increases by roughly 3 ppbv K^{-1} in the summer in the Beijing region. By 2050, climate change results in more than doubling of this slope (about 7 ppbv K^{-1}) in the same region, suggesting that ozone levels will be more sensitive to temperature changes in the future. The slope of the O_3–T_{max} relationship increases by at least 0.25 ppbv K^{-1} for the entire northern half of China, and the areas of greater slope are extended further into western China (figure 3(c)). Associated with this slope increase, we find a northward shift of the jet stream latitude, as defined by the maximum of the 500 hPa zonal wind (gray contour lines in figure 3), from 2015 to 2050. In the 2015 simulation, the jet position is approximately at 40 °N latitude (darkest gray/black contours) near the northern China border with Mongolia, but by 2050 shifts northward by about 8 °N latitude. This northward shift is also demonstrated by the differences in 500 hPa zonal wind in figure 3(c) and is associated with the projected increase in O_3–T_{max} slope in the northern part of China. This is consistent with Barnes and Fiore (2013), who found that over the Northeastern US the O_3–T_{max} slope is greatest a few degrees south of the latitude with maximum jet wind speed.

4. Ozone-related mortality over China

Using the difference in our model simulations for 2050 versus 2015 in the CLE, MFR, and CLIM scenario and concentration-response factors from a recent long-term ozone mortality study (Turner *et al* 2016), we calculate the change in annual premature mortality due to future ozone in China. Mortality calculations are completed using the equation below:

$$M = M_o \times P \times (1 - e^{-CRF \times \Delta O_3}), \qquad (1)$$

where M is the change in mortality, M_0 is the county-level baseline mortality rate for China, P is the population from the 2010 Chinese census, CRF is the concentration response factor obtained from Turner *et al* (2016), and ΔO_3 is the change in the running three-month mean of daily 1 h maximum values of surface ozone concentration between 2015 and 2050 in each scenario. Turner *et al* (2016) is chosen as a

Figure 3. Summer (JJA) sensitivity of ozone to maximum surface temperature in (a) 2015 and (b) 2050CLIM, and (c) difference. Gray contour lines show the JJA 500 hPa height zonal wind for each year and the difference.

Figure 4. (a) 2010 baseline population in China, (b) change in premature deaths between 2015 and 2050 due to climate change alone (2050CLIM scenario) (c) change in premature deaths between 2015 and 2050 due to CLE scenario (2050CLE, includes climate change), and (d) change in premature deaths between 2015 and 2050 due to MFR scenario (2050MFR, includes climate change). Units are number of deaths.

more recent estimate based on an updated cohort with a longer follow-up than previous estimates. The concentration response factor is the 'hazard ratio' as defined in Turner *et al* (2016) and is the slope of the log-linear relationship between concentration and mortality. A caveat to this calculation is that the CRF was developed from US populations. The relatively coarse model resolution may not be able to fully resolve health burden impacts at local scale. We also do not include population aging in our mortality estimates, which was recently shown to play a significant role in future mortality in China (Chen *et al* 2018). County-level baseline-mortality rates were obtained from the Chinese Center for Disease Control and Prevention.

In figure 4 we present the change in annual all-cause mortality between 2015 and 2050 due to climate change (CLIM), CLE emissions, and MFR emissions. These mortality changes are computed from the decadal average change in ozone between 2015 and 2050, and thus ignore possible transient variations in mortality that may occur in the years between. Baseline 2010 population is shown in figure 4(a). The ozone change due to climate change alone results in an additional 61 884 annual premature deaths (standard deviation of 674) in China by 2050. Not all ozone changes in the climate change scenario are statistically significant at the 95% confidence level. In the CLE scenario, which projects emissions in China to roughly stay the same or slightly increase (see figure 1 and table 1), an additional 79 786 premature deaths (standard deviation of 698) are expected. Since climate change is also a factor in the CLE scenario, this suggests that the ozone climate penalty, or the amount of ozone concentration increase due to climate change alone, makes up a significant portion of the human health burden associated with the CLE simulation, though due to climate variability, simulation results are not exactly linear. In the MFR scenario, we project that 334 822 premature deaths (standard deviation of 2880) can be avoided. Ozone changes associated with CLE and MFR are statistically significant throughout most of the entire domain. 'Though only a fraction of 1% of China's total population, this number of avoided premature deaths is a significant fraction (one-quarter to one-third) of the estimated total number of annual premature deaths attributed to ozone in present-day worldwide (1.04–1.23 million) in Malley *et al* (2017). That work utilized the same CRF from Turner *et al* (2016), which estimates a CRF of 1.02 per 10 ppbv O_3 increase, much larger than the CRF of 1.001 per 10 ppbv developed in Jerret *et al* (2009).' The largest numbers of increasing or decreasing premature deaths occur in eastern China, where both population and ozone concentrations are highest. However, in the MFR scenario, reductions in mortality extend as far west as the Sichuan province and as far south as the south China coast. Aggressive emissions reductions

will therefore have far-reaching benefits to human health, but even if ozone precursor emissions are controlled there may be a modest impact of climate change that dampens the emissions reductions benefits.

5. Discussion and conclusions

With our decades-long chemistry-climate model simulations, we investigated a range of possible futures over China under different regional and global emission scenarios. Our findings highlight the strong leverage possible over much of China by continuing to implement domestic controls on ozone precursor emissions to improve air quality in contrast to the further degradation of air quality under a scenario in which emissions continue to increase to mid-century. Premature mortality is estimated to increase in China by 2050 compared to 2015 in the CLE scenario by nearly 80 000 deaths, while emissions decreases in the MFR scenario would result in more than 330 000 avoided premature deaths. Our results show that emission controls on ozone precursor emissions as projected under the MFR scenario would largely improve air quality and health in China.

We examine non-local factors influencing future air quality over China. A sensitivity simulation in which temperatures are consistent with the high-warming RCP8.5 scenario but air pollutants and precursors remain at 2015 levels demonstrates the potential for climate change to further increase ozone and associated mortality, including via an enhanced sensitivity of ozone to temperature and a springtime enhancement of stratospheric ozone in the lower troposphere over the remote high-altitude southwestern China region in springtime. The impact of future climate change on the ability to meet air quality standards should not be overlooked, especially in southwestern China where stratospheric influence on surface air due to climate change is an important contributor to surface level ozone. Climate change may dampen future mortality benefits, as climate change alone contributes up to 62 000 premature deaths over China by 2050 compared to 2015. In addition to avoiding the worst effects of climate change in China, future mitigation of greenhouse gas emissions will have an added co-benefit of reducing air pollution-related mortality. We find that a continued rise in global emissions including over South Asia can offset some of the gains attained via controlling emissions within China alone. Our results also suggest that reductions in emissions in northern India will lead to lower ozone levels over western China. China may therefore benefit by encouraging widespread emissions reductions throughout all of Asia. Higher resolution modeling that better resolves air pollution transport at the India–China border will be important

for improved estimates of the international contribution. The use of multiple models to better assess robustness of results of a single model should also be a priority for future work. Our results imply that, as China moves to reduce its air pollution health burden, the influence from international pollution transport, especially from neighboring India, may become increasingly important for improving air quality and meeting national standards.

Acknowledgments

Data availability

Data is available on request to corresponding author.

ORCID iDs

D M Westervelt ⬥ https://orcid.org/0000-0003-0806-9961

References

Barnes E A and Fiore A M 2013 Surface ozone variability and the jet position: implications for projecting future air quality *Geophys. Res. Lett.* **40** 2839–44

Chen K, Fiore A M, Chen R, Jiang L, Jones B, Schneider A, Peters A, Bi J, Kan H and Kinney P L 2018 Future ozone-related acute excess mortality under climate and population change scenarios in China: a modeling study *PLoS Med.* **15** e1002598

Clifton O E, Fiore A M, Correa G, Horowitz L W and Naik V 2014 Twenty-first century reversal of the surface ozone seasonal cycle over the northeastern United States *Geophys. Res. Lett.* **41** 7343–50

Cohen A J *et al* 2017 Estimates and 25-year trends of the global burden of disease attributable to ambient air pollution: an analysis of data from the Global Burden of Diseases Study 2015 *Lancet* **389** 1907–18

Donner L J *et al* 2011 The dynamical core, physical parameterizations, and basic simulation characteristics of the atmospheric component AM3 of the GFDL global coupled model CM3 *J. Clim.* **24** 3484–519

Fiore A M *et al* 2012 Global air quality and climate *Chem. Soc. Rev.* **41** 6663

Fiore A M, Naik V and Leibensperger E M 2015 Air quality and climate connections *J. Air Waste Manage. Assoc.* **65** 645–85

Jacob D J and Winner D A 2009 Effect of climate change on air quality *Atmos. Environ.* **43** 51–63

Jerrett M, Burnett R T, Pope C A, Ito K, Thurston G, Krewski D, Shi Y L, Calle E and Thun M 2009 Long-term ozone exposure and mortality *New Engl. J. Med.* **360** 1085–95

Jhun I, Fann N, Zanobetti A and Hubbell B 2014 Effect modification of ozone-related mortality risks by temperature in 97 US cities *Environ. Int.* **73** 128–34

Kirtman B *et al* 2013 Near-term climate change: projections and predictability *Climate Change 2013: The Physical Science Basis, Contribution of Working Group I to the Fifth Assessment Report of the Intergovernmental Panel on Climate Change* (New York: Cambridge University Press) pp 953–1028

Langford A O, Aikin K C, Eubank C S and Williams E J 2009 Stratospheric contribution to high surface ozone in Colorado during springtime *Geophys. Res. Lett.* **36** L12801

Li K, Jacob D J, Liao H, Shen L, Zhang Q and Bates K H 2018 Anthropogenic drives of 2013–2017 trends in summer surface ozone in China *Proc. Natl Acad. Sci.* **116** 422–7

Lin M, Fiore A M, Cooper O R, Horowitz L W, Langford A O, Levy H, Johnson B J, Naik V, Oltmans S J and Senff C J 2012 Springtime high surface ozone events over the western United States: quantifying the role of stratospheric intrusions *J. Geophys. Res. Atmos.* **117** D00V22

Lin M, Fiore A M, Horowitz L W, Langford A O, Oltmans S J, Tarasick D and Rieder H E 2015 Climate variability modulates western US ozone air quality in spring via deep stratospheric intrusions *Nat. Commun.* **6** 7105

Liu F, Beirle S, Zhang Q, van der R J A, Zheng B, Tong D and He K 2017 NOx emission trends over Chinese cities estimated from OMI observations during 2005 to 2015 *Atmos. Chem. Phys.* **17** 9261–75

Liu Q, Lam K S, Jiang F, Wang T J, Xie M, Zhuang B L and Jiang X Y 2013 A numerical study of the impact of climate and emission changes on surface ozone over South China in autumn time in 2000–2050 *Atmos. Environ.* **76** 227–37

Malley C S, Henze D K, Kuylenstierna J C I, Vallack H W, Davila Y, Anenberg S C, Turner M C and Ashmore M R 2017 Updated global estimates of respiratory mortality in adults ⩾30 years of age attributable to longterm ozone exposure *Environ. Health Perspect.* **125** 1390

Myhre G *et al* 2013 Anthropogenic and Natural Radiative Forcing *Climate Change 2013, The Physical Science Basis, Contribution of Working Group I to the Fifth Assessment Report of the Intergovernmental Panel on Climate Change* ed T F Stocker *et al* (Cambridge: Cambridge University Press)

O'Neill B C *et al* 2016 The scenario model intercomparison project (ScenarioMIP) for CMIP6 *Geosci. Model Dev.* **9** 3461–82

Prather M J, Zhu X, Tang Q, Hsu J and Neu J L 2011 An atmospheric chemist in search of the tropopause *J. Geophys. Res.* **116** D04306

Rasmussen D J, Fiore A M, Naik V, Horowitz L W, McGinnis S J and Schultz M G 2012 Surface ozone-temperature relationships in the eastern US: a monthly climatology for evaluating chemistry-climate models *Atmos. Environ.* **47** 142–53

Rieder H E, Fiore A M, Horowitz L W and Naik V 2015 Projecting policy-relevant metrics for high summertime ozone pollution events over the eastern United States due to climate and emission changes during the 21st century *J. Geophys. Res. Atmos.* **120** 784–800

Stohl A *et al* 2015 Evaluating the climate and air quality impacts of short-lived pollutants *Atmos. Chem. Phys.* **15** 10529–66

Tai A P K, Martin M V and Heald C L 2014 Threat to future global food security from climate change and ozone air pollution *Nat. Clim. Change* **4** 817–21

Task Force on Hemispheric of Air Pollution 2010 Hemispheric transport of air pollution 2010 *Part A: Ozone and Particulate Matter, Air Pollution Studies No. 17* (United Nations Economic Commission for Europe, 2010) ed F Dentener (New York: United Nations)

Turner M C *et al* 2016 Long-term ozone exposure and mortality in a large prospective study *Am. J. Respir. Crit. Care Med.* **193** 1134–42

Wang S X *et al* 2014 Emission trends and mitigation options
for air pollutants in East Asia *Atmos. Chem. Phys.* **14**
6571–603

Wang Y, Shen L, Wu S, Mickley L, He J and Hao J 2013 Sensitivity
of surface ozone over China to 2000–2050 global
changes of climate and emissions *Atmos. Environ.* **75**
374–82

Yue X and Unger N 2014 Ozone vegetation damage effects on gross
primary productivity in the United States *Atmos. Chem. Phys.*
14 9137–53

Zhu J and Liao H 2016 Future ozone air quality and radiative forcing
over China owing to future changes in emissions under the
Representative Concentration Pathways (RCPs) *J. Geophys.
Res. Atmos.* **121** 1978–2001

Supplementary information for…
Mid-21st century ozone air quality and health burden in China under emissions scenarios and climate change

D.M. Westervelt[a,b], C.T. Ma[c], M.Z. He[d], A.M. Fiore[a,e], P.L. Kinney[f], M.-A. Kioumourtzoglou[d], S. Wang[g], J. Xing[g], D. Ding[g], G. Correa[a]

1 Previous literature

Numerous studies have investigated the global impact of anthropogenic emissions and climate on surface ozone (Dentener et al., 2006; Fiore et al., 2015; Jacob and Winner, 2009; Kim et al., 2015; Langner et al., 2012; Lapina et al., 2015; Liao et al., 2006; Racherla and Adams, 2006, 2009, Stevenson et al., 2013, 2006; Tagaris et al., 2007; Wu et al., 2008a, 2008b; Young et al., 2013) without necessarily focusing exclusively on China or East Asia. Generally, these studies projected an increase of a few ppbv for global mean surface ozone due to future climate changes alone by mid-century compared to present-day, with decreases in remote region and increases over heavily populated areas in China (Zhu and Liao, 2016). Projected changes in ozone are highly dependent on choice of scenario for precursor emissions. For example, older studies that utilized the Special Report on Emissions Scenarios (SRES) generally projected increases in global mean surface ozone (Brasseur et al., 2006; Dentener et al., 2006), while more recent studies using the Representative Concentration Pathways (RCP) resulted in ozone decreases due to strong projected reductions in precursor emissions (Fiore et al., 2012; Szopa et al., 2013; Young et al., 2013).

2. Model Description

We use the atmospheric component of the NOAA Geophysical Fluid Dynamics Laboratory climate model (GFDL-AM3) to perform simulations of present and future climate under different emissions scenarios. We employ the C48 horizontal resolution, which uses a finite-volume cubed-sphere horizontal grid consisting of 6 faces of 48 grid cells along each edge, resulting in roughly a 200-km by 200-km spatial resolution. The vertical grid consists of 48 levels extending from the surface up to about 0.01 hPa (80 km). Transport of tracers uses the finite volume algorithm of Lin and Rood (1996) with updates as described by Putman and Lin (2007) and Donner et al. (2011). Anthropogenic emissions are prescribed by the ECLIPSE inventory and will be discussed in section 2.2. Tropospheric chemistry for gas-phase species follows the work of Horowitz et al. (2003) and Horowitz (2006), which solves differential equations of reaction rates using an implicit Euler backward method solver with Newton-Raphson iteration. Further model description and evaluation details can be found in Donner et al. (2011), Naik et al. (2013), and references therein.

3 Emissions

We use the IIASA ECLIPSE (Evaluating the Climate and Air Quality Impacts of Short-Lived Pollutants) v5a gridded emissions of SO_2, NOx, NH_3, NMVOC, BC, OC, $PM_{2.5}$, PM_{10}, and CO in the current legislation (CLE) and maximum technically feasible reduction (MFR) future emissions scenarios for 2050 (Stohl et al., 2015). The ECLIPSE emissions scenarios are developed from the GAINS model (Greenhouse gas-Air pollution Interactions with Synergies) which uses information about emissions sources, environmental polices, mitigation potential, projections of energy use, industrial activity, and agricultural processes to provide emissions of short-lived air pollutants and long-lived greenhouse gases (Amann et al., 2011). CLE contains all present and planned environmental laws assuming full enforcement in the future, while MFR is a mitigation scenario based on all available advanced emission control technologies. As previously described, this version of ECLIPSE includes improvements over previous emissions inventories such as SRES and RCP, specifically to ozone precursor emissions (including NO_x) in China. We use year 2015 CLE emissions as our baseline year. Emissions are provided every 5 to 10 years with monthly time resolution from 1990 to 2050 at 0.5 by 0.5 degree latitude by longitude grid, though we only use 2015 and 2050 in this work.

Natural emissions of soil NO_x, and lightning NO_x are described by Naik et al. (2013). The Model of Emissions of Gases and Aerosols from Nature (MEGAN) is implemented for interactive isoprene emissions, which are responsive to meteorology and thus future climate change (Guenther et al., 2006; Rasmussen et al., 2012). Concentrations of long-lived greenhouse gases, including methane, are based on Meinshausen et al. (2011).

4 Model evaluation

The atmospheric physics and dynamics simulated in the GFDL-AM3 model were first described and evaluated by Donner et al. (2011). Its chemistry and the inclusion of troposphere-stratosphere interactions, gas-aerosol chemistry, and aerosol-cloud interactions (including direct and indirect aerosol radiative effects), were evaluated by Naik et al. (2013). In particular, for ozone, Naik et al. (2013) find that the seasonal cycle is well-represented by the model in the lower troposphere in northern midlatitudes, and similarly at southern hemisphere tropical and midlatitudes. Specific comparisons of observed and GFDL-AM3 model-simulated surface ozone concentrations over China have not previously been performed.

We use hourly observations of surface ozone concentrations from the Chinese national air quality monitoring network, which was developed after the 2012 adoption of the new National Ambient Air Quality Standard GB 3095-2012. Data is collected continuously on an hourly basis, and all values are recorded at Beijing Local Time (UTC+8). Air quality stations are clustered in urban areas, with several to a dozen sites per city in the east. In the west, fewer cities have monitoring networks in place, and sites tend to be more widely distributed. Various statistical analyses have been conducted previously for other subsets of air quality data obtained from this network (Rohde and Muller, 2015; Zhang and Cao, 2015). Consistent with prior studies, Rohde and Muller (2015) find during their four-month analysis period beginning in April of 2014 that the greatest air pollution (including NO_x and ozone) occurs in population centers of eastern China, with modest

levels (<65 ppbv) across northern and central China, not limited to major cities or geologic basins.

There are 1494 monitoring stations in 364 cities across China during the period from 1 Jan 2015 to 31 Dec 2015, for evaluation against our base-year of 2015 AM3 model simulations. Both the model and observations are converted to maximum daily 8-hour average values (MDA8). In Figure 2, we compare modeled and observed monthly mean surface ozone concentrations in 12 Chinese cities by sampling AM3 at the corresponding grid cell. These 12 cities represent a diverse set of urban geographical locations throughout China. The model seasonal cycle (red line) agrees well with the citywide observed mean (black lines), with correlation coefficients as high as 0.95 in Beijing, for example. The model is biased high at most cities throughout the year compared to the citywide mean by anywhere from 12.9 ppbv (Lanzhou) to 21.8 ppbv (Harbin). However, in several cities, there is agreement between the model and at least one observation site (grey lines in Fig. S4) during a certain time of year. For example, in Shijiazhuang (Fig. S4b), the observed summertime MDA8 ozone at several sites matches with the model at about 85 ppbv. For Guangzhou and Lanzhou (Figs S4e and S4l), modeled MDA8 ozone is in agreement with several observation sites almost throughout most of the year, around 50-60 ppbv for both locations. Generally, the model exhibits large biases in cities in the northeastern half of China including Harbin (21.7 ppbv positive bias), Beijing (18.7 ppbv positive pias), and Nanjing (20.3 ppbv positive bias). Lower model biases occur in southern half of China (e.g. Guangzhou, 15.3 ppbv; Fuzhou, 13.3 ppbv) and western China (Lanzhou, 12.9 ppbv). The largest biases in major cities such as Shanghai, Beijing, and Nanjing occur during the summer months. This positive summertime bias is not unique to the GFDL-AM3 model over China and has been documented over the Eastern United States by Rieder et al. (2015) and for other models in Fiore et al. (2009), Pfister et al. (2014), and Rasmussen et al. (2012). In particular, Fiore et al. (2009) found a multimodel mean bias greater than 12 ppbv over Japan and 14 ppbv over the eastern US in the summer months. Since long-term surface ozone measurements throughout China have only recently become widely and publicly available, estimation of model biases specifically over China are currently not well characterized and often limited to few sites.

There are several possible explanations for the model bias over these Chinese cities. The summer bias may be related to uncertainties in emissions of both anthropogenic and biogenic precursors, as well as uncertainties in ozone sinks such as dry deposition. The version of GFDL-AM3 presented here uses static, monthly mean values of ozone dry deposition velocity taken from the GEOS-Chem model (Naik et al., 2012). Recently, implementing a new treatment of ozone dry deposition coupled to the dynamic vegetation land model into a newer version of GFDL-AM3 was found to reduce summertime bias in modeled surface ozone by as much as 5-10 ppbv over China (Clifton, 2018). The coarse horizontal spatial resolution (~200 by 200 km) cannot resolve ozone titration chemistry (fresh NO emissions react with ozone to form NO_2) at local scales. Coarse models cannot reproduce highly localized hotspots of NO_x that exist in observations, due to dilution spread over a large model grid box. This underestimation of NO_x therefore causes an overestimate in ozone, as ozone is not titrated as frequently with NO in the model. Urumqi, a city with a population of 3.5 million people in far northwest China, has a positive model bias of 20.5 ppbv, most of which occurs during the winter months when observed monthly mean MDA8 ozone falls below 10 ppbv due to titration. Similar ozone

concentrations and biases are seen in Chengdu in the winter, where observed ozone concentrations lower than 20 ppbv are not reproduced by AM3. Titration chemistry of NO_x and ozone has been shown to be difficult to reproduce in both regional and global models (Chatani et al., 2014; Engardt, 2008; Pommier et al., 2018).

Figure S4 shows the seasonal mean MDA8 surface ozone concentrations in the GFDL-AM3 model for 2015 over China. Modeled ozone concentrations in 2015 peak in the summer months (JJA), with the highest values over eastern China reaching 100 ppbv. Concentrations of surface ozone are at minimum in the winter months (DJF) over eastern China, but are elevated over the Tibetan Plateau (southwestern China). Ozone in western China is highest in springtime.

5 Correlation between temperature and ozone changes

We investigate the relationship between daily changes in MDA8 and changes in maximum daily surface temperature between 2015 and 2050 by season in 2050CLIM (Figure S13). Each correlation contains 10 years of ~92 daily MDA8 ozone or maximum temperatures (3 months) for a total of ~920 data points per season. Over much of China throughout the year, especially in summer, changes in daily maximum ozone are strongly correlated to changes in surface temperature (r > 0.6). Changes in ozone and temperature are not correlated over the Tibetan Plateau where stratospheric influence dominates; the anti-correlation is consistent with the association of cold, dry descending air masses with higher ozone (Langford and Reid, 1998).
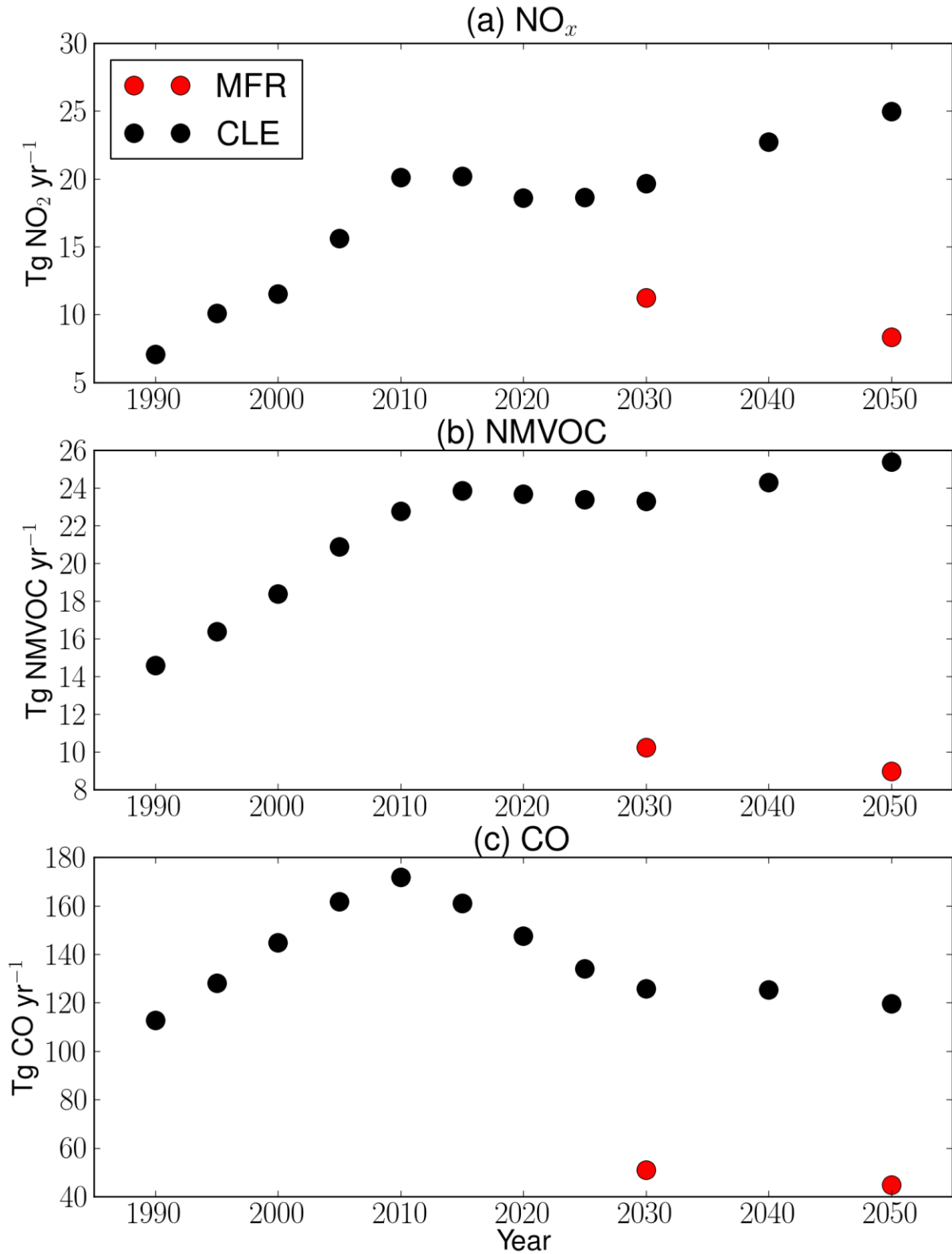
Figure S1: Emissions of ozone precursors (a) NOx, (b) NMVOC, and (c) CO from 1990-2050 in the ECLIPSE CLE and MFR scenario over China
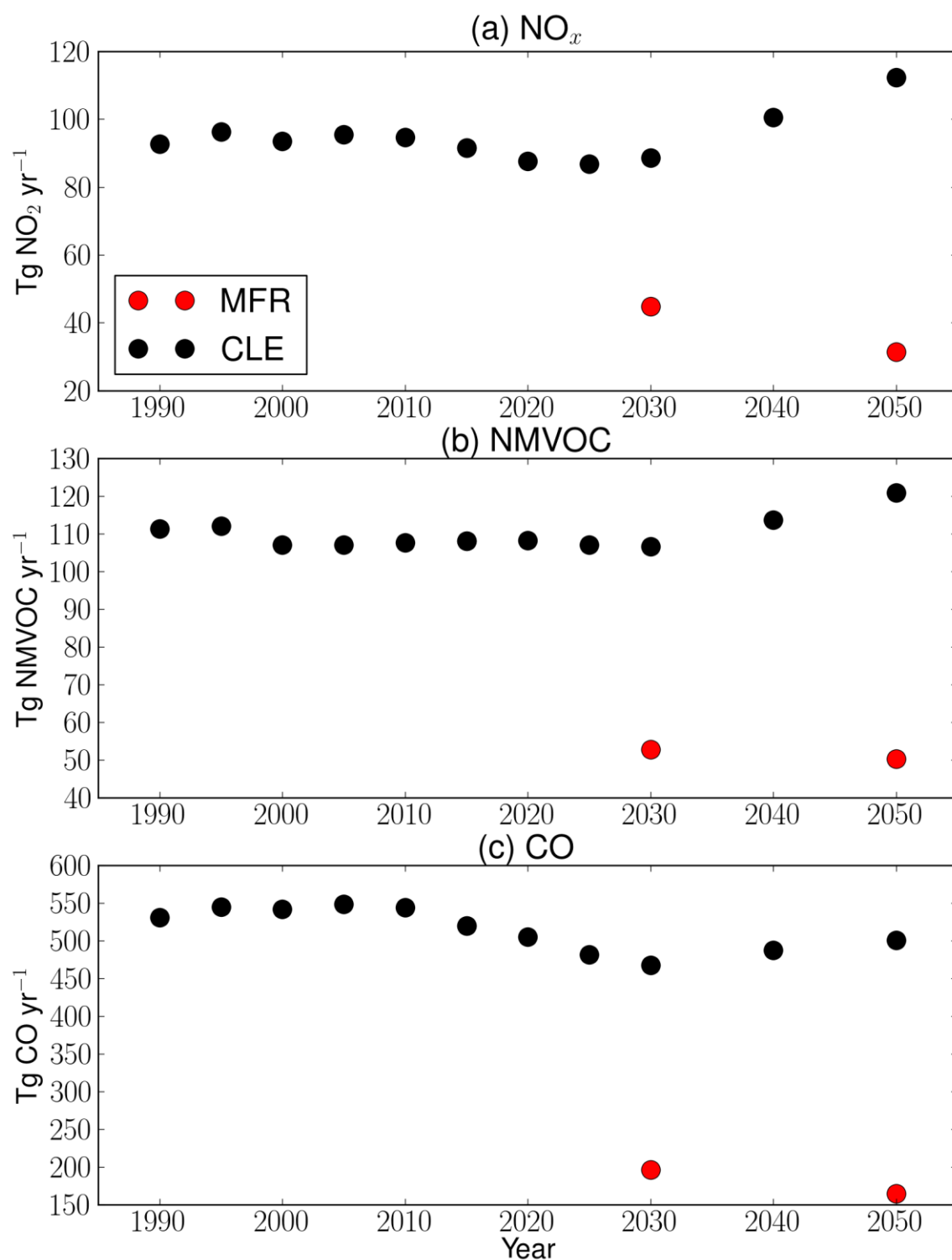
Figure S2: Global emissions of ozone precursors (a) NOx, (b) NMVOC, and (c) CO from 1990-2050 in the ECLIPSE CLE and MFR scenario
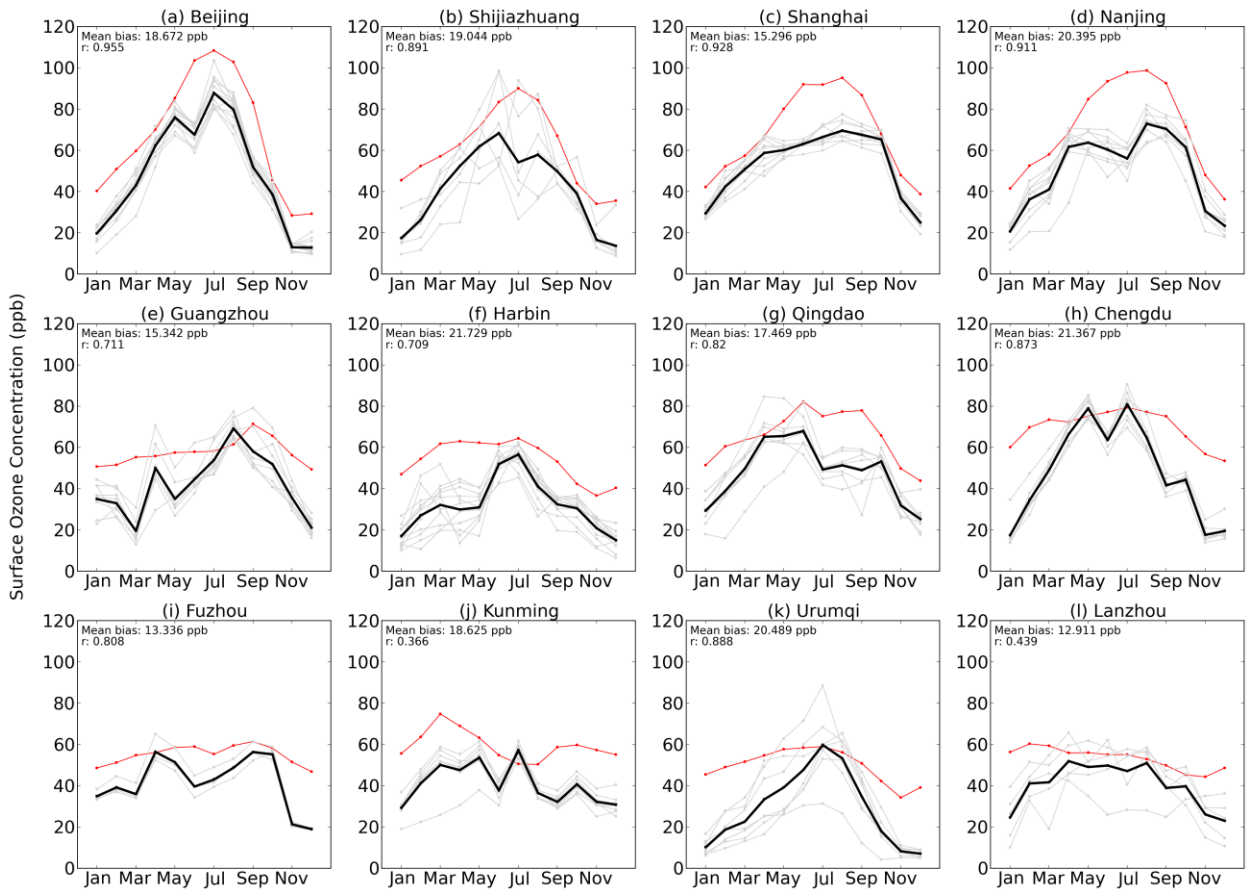
Figure S3: Monthly mean MDA8 surface ozone concentration (ppbv) at 12 urban areas in China (individual stations in grey; multi-station mean in black), and the decadal mean monthly averages sampled at the GFDL-AM3 model grid cell corresponding to the location of the measurement site (red). Observations are for year 2015 only.
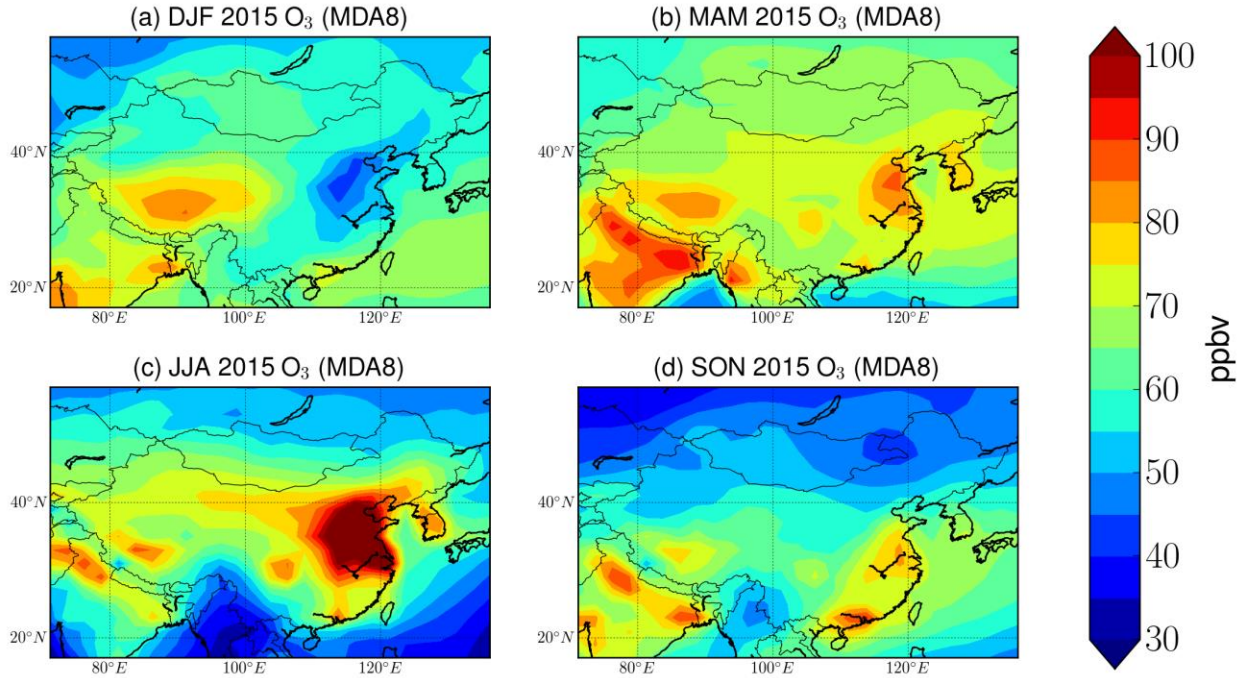
Figure S4: Decadal mean of the maximum daily 8-hour average ozone (MDA8) by season (a) DJF, (b) MAM, (c) JJA, (d) SON in the present-day GFDL AM3 simulations with repeated 2015 conditions.
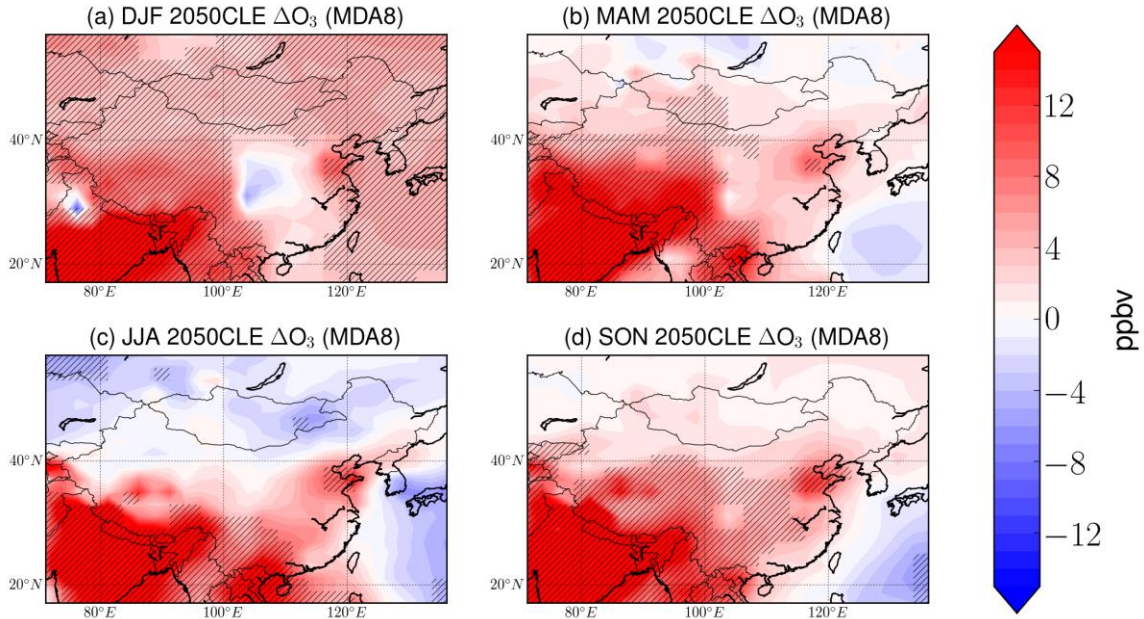
Figure S5: Change from 2015 to 2050 in decadal average maximum daily 8-hour average ozone (MDA8) in the GFDL AM3 simulation 2050CLE during (a) DJF, (b) MAM, (c) JJA, (d) SON. Hatching represents statistical significance at 95% confidence level.
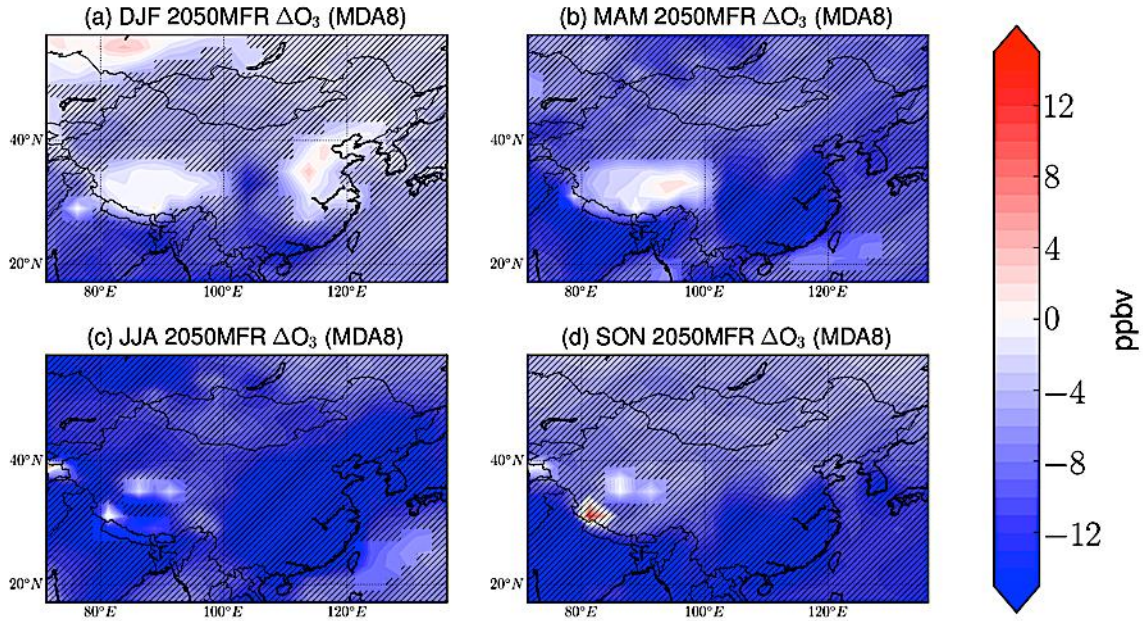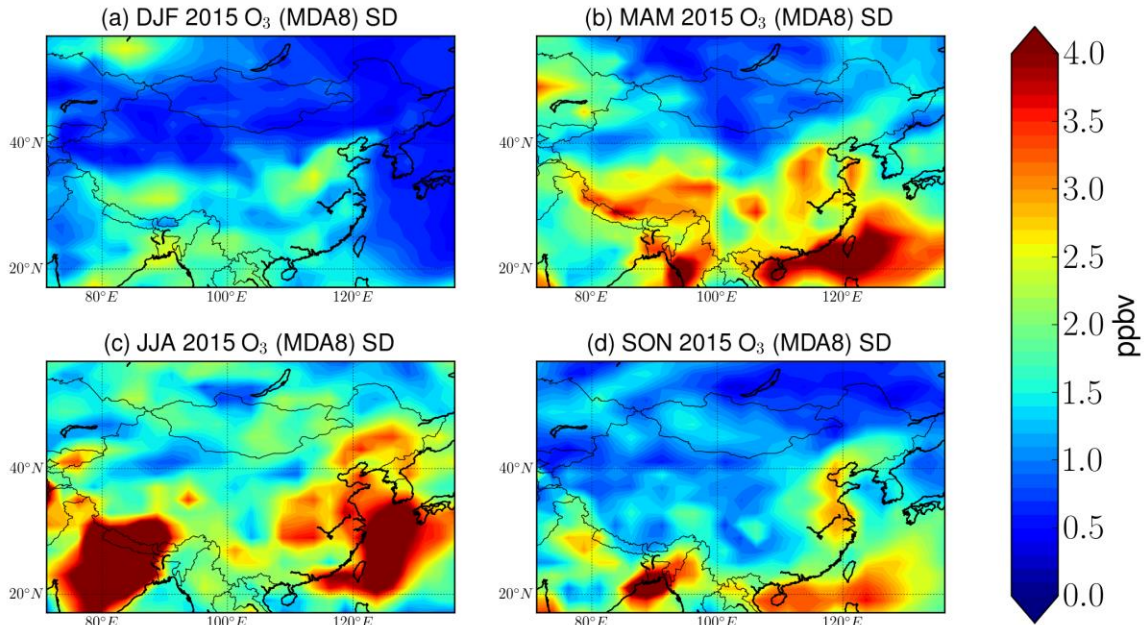
Figure S6: Change from 2015 to 2050 in decadal average maximum daily 8-hour average ozone (MDA8) in the GFDL AM3 simulation 2050MFR during (a) DJF, (b) MAM, (c) JJA, (d) SON. Hatching represents statistical significance at 95% confidence level.

Figure S7: Standard deviation of MDA8 surface ozone in present-day 2015 simulations for (a) DJF, (b) MAM, (c) JJA, and (d) SON. Standard deviations are shown for 10-year simulations with repeated 2015 conditions
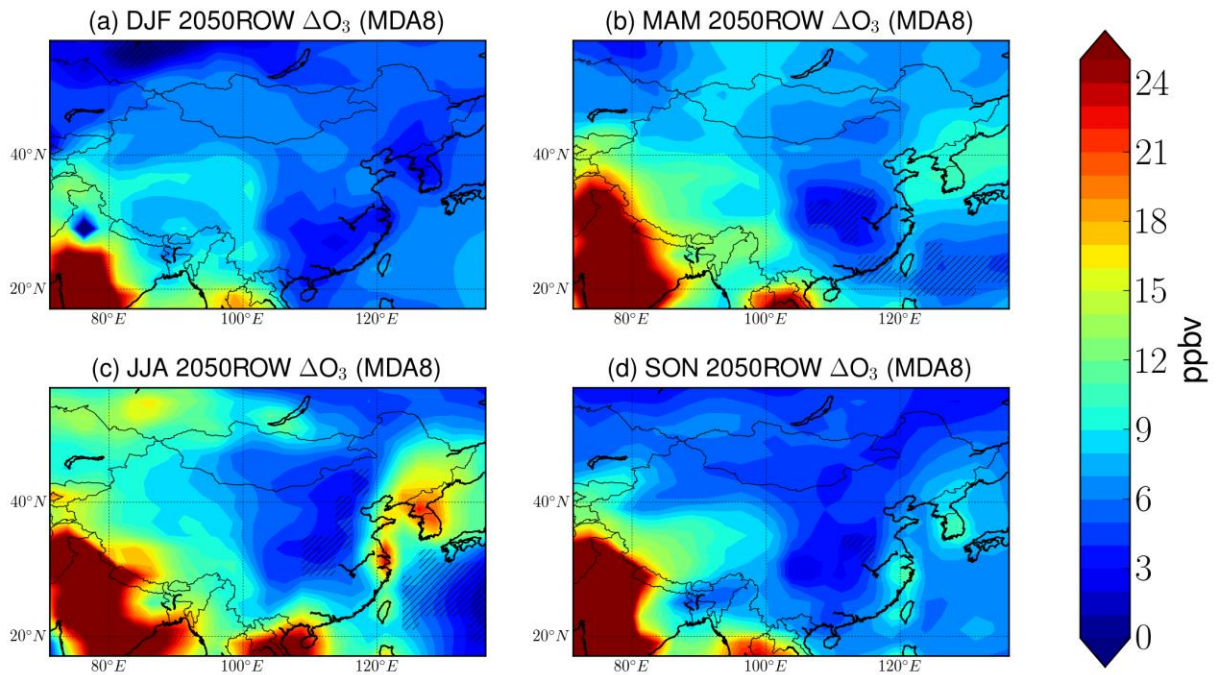

Figure S8: Change in surface MDA8 ozone if only China follows the MFR scenario but the rest of the world follows the higher-emitting CLE scenario (2050ROW, Rest of World) in (a) DJF, (b) MAM, (c) JJA, and (d) SON. For clarity of visualization, areas without hatching represent statistical significance.
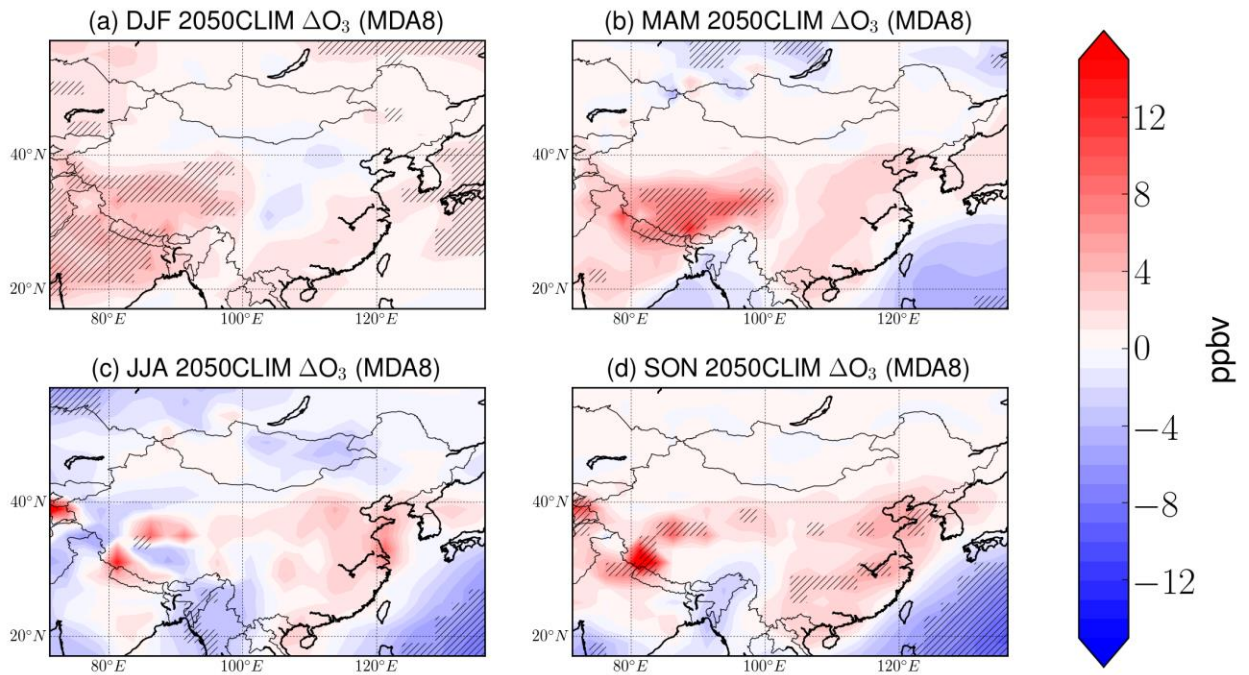
Figure S9: Change from 2015 to 2050 in decadal average maximum daily 8-hour average ozone (MDA8) in the GFDL AM3 simulation 2050CLIM during (a) DJF, (b) MAM, (c) JJA, (d) SON. Hatching represents statistical significance at 95% confidence level.
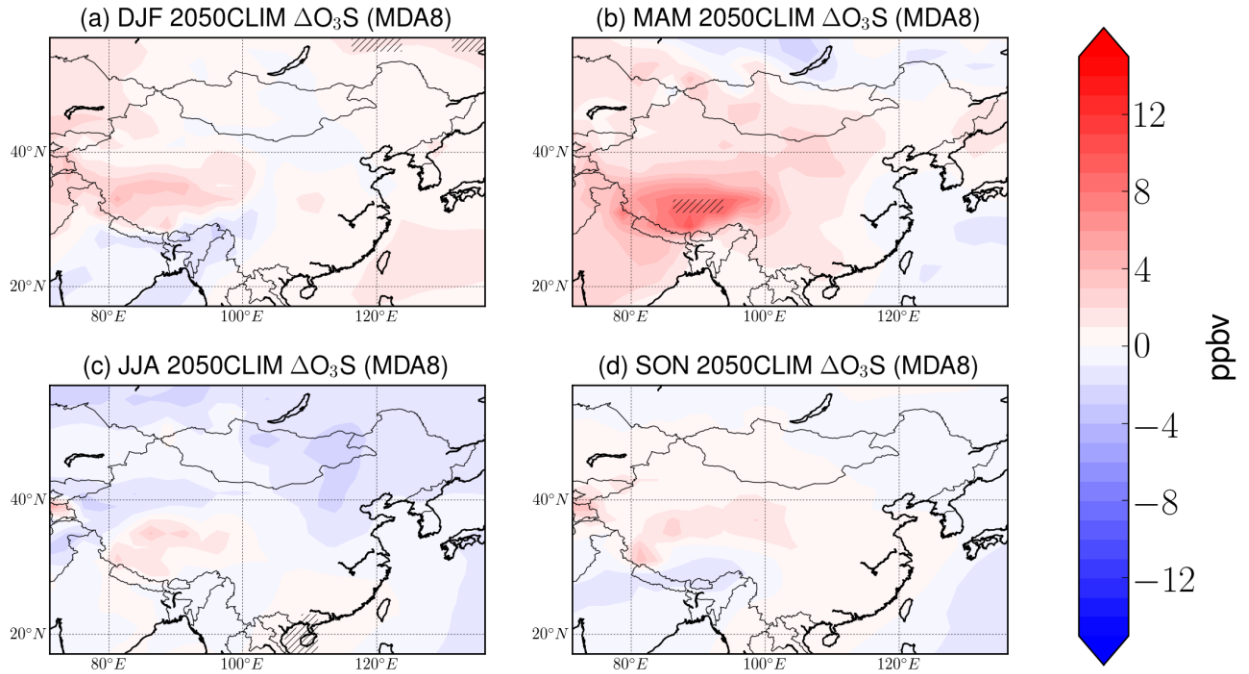
Figure S10: Change from 2015 to 2050 in the contribution of stratospheric ozone to surface decadal average maximum daily 8-hour average ozone (MDA8) in the GFDL-AM3 simulation 2050CLIM for (a) DJF, (b) MAM, (c) JJA, (d) SON. All values were averaged over 10 years of repeated 2015 or 2050 conditions. Hatching represents statistical significance at 95% confidence level.
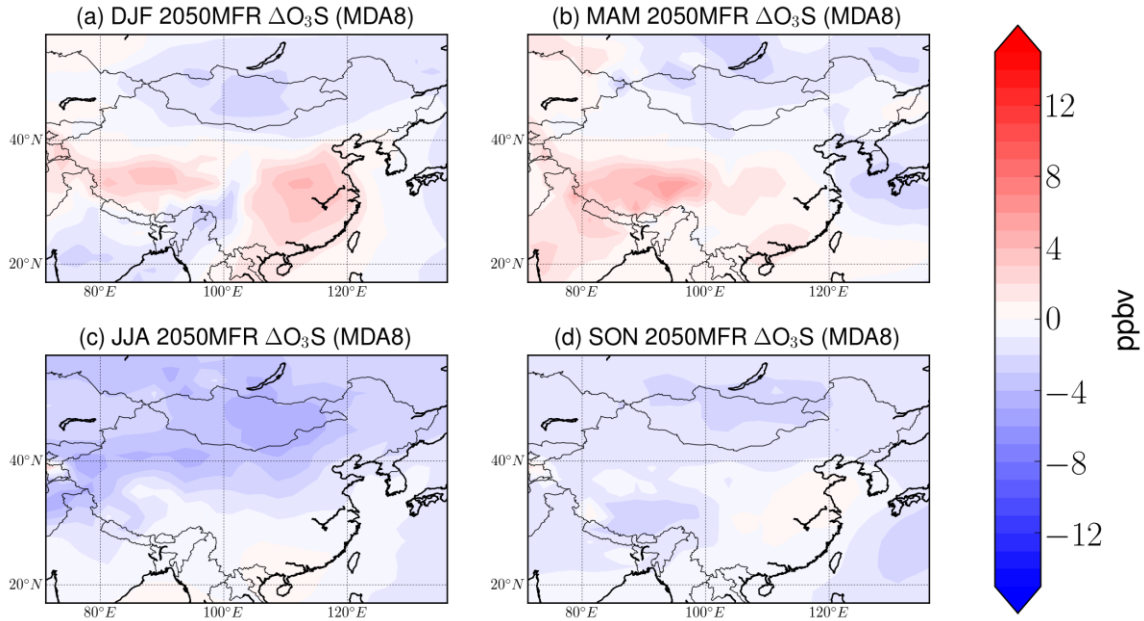
Figure S11: Change from 2015 to 2050 in the contribution of stratospheric ozone to surface decadal average maximum daily 8-hour average ozone (MDA8) in the GFDL-AM3 simulation 2050MFR for (a) DJF, (b) MAM, (c) JJA, (d) SON. All values were averaged over 10 years of repeated 2015 or 2050 conditions. Hatching represents statistical significance at 95% confidence level.
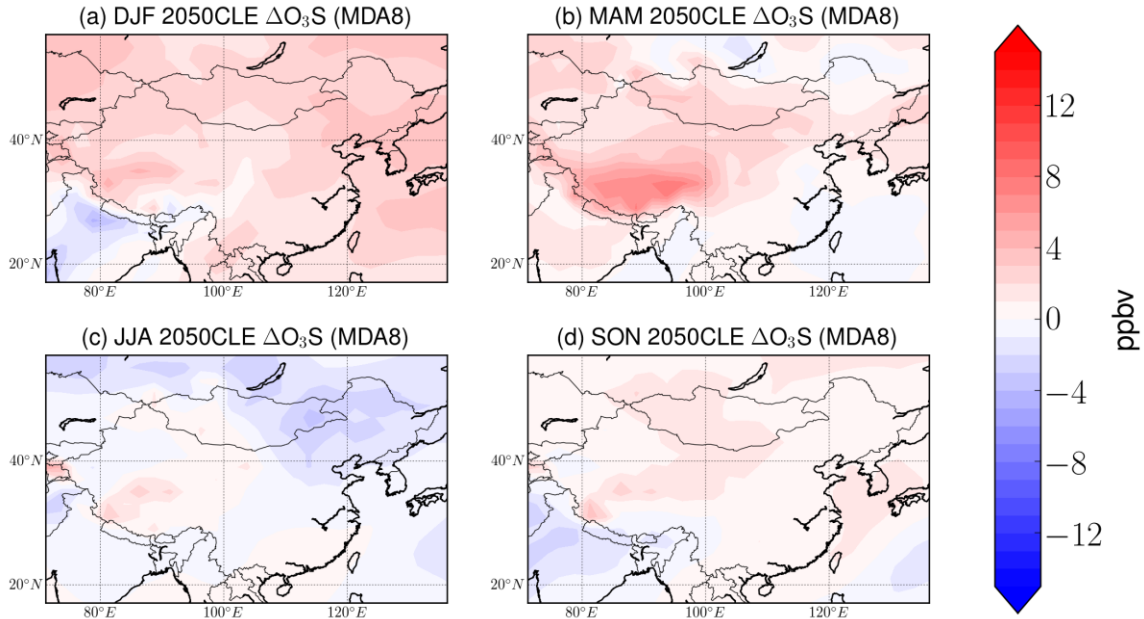
Figure S12: Change from 2015 to 2050 in the contribution of stratospheric ozone to surface decadal average maximum daily 8-hour average ozone (MDA8) in the GFDL-AM3 simulation 2050CLE for (a) DJF, (b) MAM, (c) JJA, (d) SON. All values were averaged over 10 years of repeated 2015 or 2050 conditions. Hatching represents statistical significance at 95% confidence level.
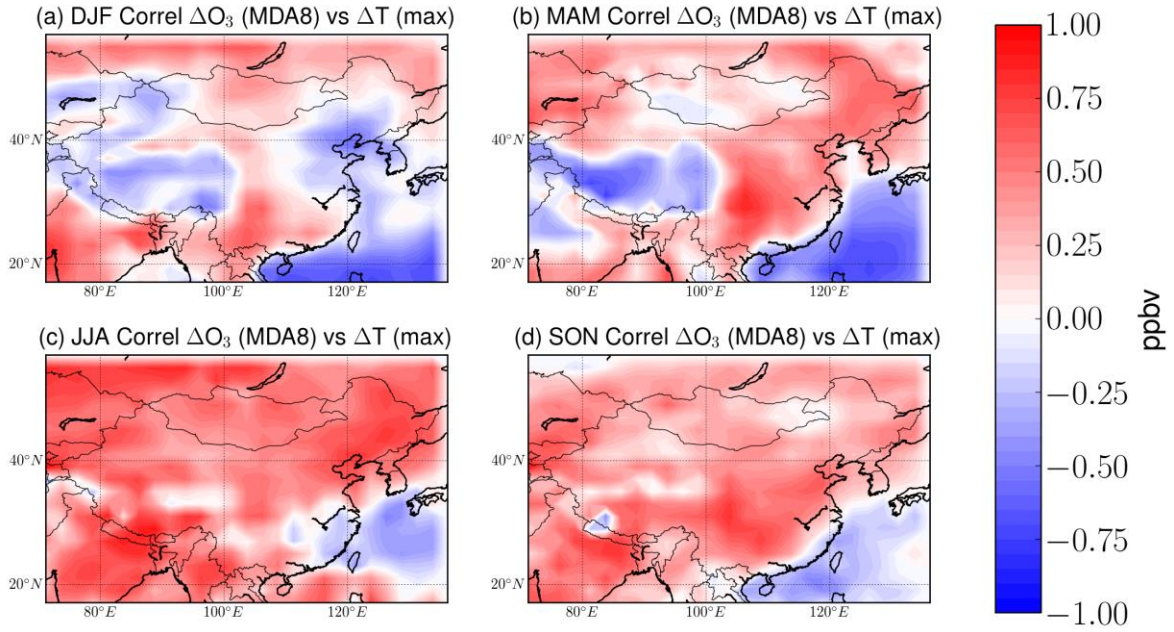
Figure S13: Correlation between change in maximum 2 meter reference temperature and change in maximum daily 8-hour average ozone (MDA8) between 2050 in the CLIM scenario and 2015 for (a) DJF, (b) MAM, (c) JJA, and (d) SON.

References

Amann, M., Bertok, I., Borken-Kleefeld, J., Cofala, J., Heyes, C., Höglund-Isaksson, L., Klimont, Z., Nguyen, B., Posch, M., Rafaj, P., Sandler, R., Schöpp, W., Wagner, F. and Winiwarter, W.: Cost-effective control of air quality and greenhouse gases in Europe: Modeling and policy applications, Environ. Model. Softw., 26(12), 1489–1501, doi:10.1016/J.ENVSOFT.2011.07.012, 2011.

Brasseur, G. P., Schultz, M., Granier, C., Saunois, M., Diehl, T., Botzet, M., Roeckner, E. and Walters, S.: Impact of Climate Change on the Future Chemical Composition of the Global Troposphere, J. Clim., 19(16), 3932–3951, doi:10.1175/JCLI3832.1, 2006.

Chatani, S., Amann, M., Goel, A., Hao, J., Klimont, Z., Kumar, A., Mishra, A., Sharma, S., Wang, S. X., Wang, Y. X. and Zhao, B.: Photochemical roles of rapid economic growth and potential abatement strategies on tropospheric ozone over South and East Asia in 2030, Atmos. Chem. Phys., 14(17), 9259–9277, doi:10.5194/acp-14-9259-2014, 2014.

Dentener, F., Stevenson, D., Ellingsen, K., van Noije, T., Schultz, M., Amann, M., Atherton, C., Bell, N., Bergmann, D., Bey, I., Bouwman, L., Butler, T., Cofala, J., Collins, B., Drevet, J., Doherty, R., Eickhout, B., Eskes, H., Fiore, A., Gauss, M., Hauglustaine, D., Horowitz, L., Isaksen, I. S. A., Josse, B., Lawrence, M., Krol, M., Lamarque, J. F., Montanaro, V., Müller, J. F., Peuch, V. H., Pitari, G., Pyle, J., Rast, S., Rodriguez, J., Sanderson, M., Savage, N. H., Shindell, D., Strahan, S., Szopa, S., Sudo, K., Van Dingenen, R., Wild, O. and Zeng, G.: The Global Atmospheric Environment for the Next Generation, Environ. Sci. Technol., 40(11), 3586–3594, doi:10.1021/es0523845, 2006.

Donner, L. J., Wyman, B. L., Hemler, R. S., Horowitz, L. W., Ming, Y., Zhao, M., Golaz, J.-C., Ginoux, P., Lin, S.-J., Schwarzkopf, M. D., Austin, J., Alaka, G., Cooke, W. F., Delworth, T. L., Freidenreich, S. M., Gordon, C. T., Griffies, S. M., Held, I. M., Hurlin, W. J., Klein, S. a., Knutson, T. R., Langenhorst, A. R., Lee, H.-C., Lin, Y., Magi, B. I., Malyshev, S. L., Milly, P. C. D., Naik, V., Nath, M. J., Pincus, R., Ploshay, J. J., Ramaswamy, V., Seman, C. J., Shevliakova, E., Sirutis, J. J., Stern, W. F., Stouffer, R. J., Wilson, R. J., Winton, M., Wittenberg, A. T. and Zeng, F.: The Dynamical Core, Physical Parameterizations, and Basic Simulation Characteristics of the Atmospheric Component AM3 of the GFDL Global Coupled Model CM3, J. Clim., 24(13), 3484–3519, doi:10.1175/2011JCLI3955.1, 2011.

Engardt, M.: Modelling of near-surface ozone over South Asia, J. Atmos. Chem., 59(1), 61–80, doi:10.1007/s10874-008-9096-z, 2008.

F. Dentener, *,†, D. Stevenson, ‡, K. Ellingsen, §, T. van Noije, ‖, M. Schultz, ¶, M. Amann, ⊥, C. Atherton, ×., N. Bell, ∇, D. Bergmann, ×., I. Bey, ○, L. Bouwman, #, T. Butler, +, J. Cofala, ⊥, B. Collins, ·, J. Drevet, ○, R. Doherty, ‡, B. Eickhout, #, H. Eskes, ‖, A. Fiore, ∞, M. Gauss, §, D. Hauglustaine, ◇, L. Horowitz, ∞, I. S. A. Isaksen, §, B. Josse, ★, M. Lawrence, +, M. Krol, †, J. F. Lamarque, ◇, V. Montanaro, @, J. F. Müller, ◆, V. H. Peuch, ★, G. Pitari, @, J. Pyle, £, S. Rast, ¶, J. Rodriguez, °,¢, M. Sanderson, ·, N. H. Savage, £, D. Shindell, ∇, S. Strahan, ᐞ, S. Szopa, ◇, K. Sudo, ✗, R. Van Dingenen, †, O. Wild, ✗ and and Zeng£, G.: The Global Atmospheric Environment for the Next Generation, , doi:10.1021/ES0523845, 2006.

Fiore, A. M., Dentener, F. J., Wild, O., Cuvelier, C., Schultz, M. G., Hess, P., Textor, C., Schulz, M., Doherty, R. M., Horowitz, L. W., MacKenzie, I. A., Sanderson, M. G., Shindell, D. T., Stevenson, D. S., Szopa, S., Van Dingenen, R., Zeng, G., Atherton, C., Bergmann, D., Bey, I., Carmichael, G., Collins, W. J., Duncan, B. N., Faluvegi, G., Folberth, G., Gauss, M., Gong, S., Hauglustaine, D., Holloway, T., Isaksen, I. S. A., Jacob, D. J., Jonson, J. E., Kaminski, J. W., Keating, T. J., Lupu, A., Marmer, E., Montanaro, V., Park, R. J., Pitari, G., Pringle, K. J., Pyle, J. A., Schroeder, S., Vivanco, M. G., Wind, P., Wojcik, G., Wu, S. and Zuber, A.: Multimodel estimates of intercontinental source-receptor relationships for ozone pollution, J. Geophys. Res., 114(D4), D04301, doi:10.1029/2008JD010816, 2009.

Fiore, A. M., Naik, V., Spracklen, D. V., Steiner, A., Unger, N., Prather, M., Bergmann, D., Cameron-Smith, P. J., Cionni, I., Collins, W. J., Dalsøren, S., Eyring, V., Folberth, G. A., Ginoux, P., Horowitz, L. W., Josse, B., Lamarque, J.-F., MacKenzie, I. A., Nagashima, T., O'Connor, F. M., Righi, M., Rumbold, S. T., Shindell, D. T., Skeie, R. B., Sudo, K., Szopa, S., Takemura, T. and Zeng, G.: Global air quality and climate, Chem. Soc. Rev., 41(19), 6663, doi:10.1039/c2cs35095e, 2012.

Fiore, A. M., Naik, V. and Leibensperger, E. M.: Air Quality and Climate Connections, J. Air Waste Manage. Assoc., 65(6), 645–685, doi:10.1080/10962247.2015.1040526, 2015.

Guenther, A., Karl, T., Harley, P., Wiedinmyer, C., Palmer, P. I. and Geron, C.: Estimates of global terrestrial isoprene emissions using MEGAN (Model of Emissions of Gases and Aerosols from Nature), Atmos. Chem. Phys., 6(11), 3181–3210, doi:10.5194/acp-6-3181-2006, 2006.

Horowitz, L. W.: Past, present, and future concentrations of tropospheric ozone and aerosols: Methodology, ozone evaluation, and sensitivity to aerosol wet removal, J. Geophys. Res., 111(D22), D22211, doi:10.1029/2005JD006937, 2006.

Horowitz, L. W., Walters, S., Mauzerall, D. L., Emmons, L. K., Rasch, P. J., Granier, C., Tie, X., Lamarque, J.-F., Schultz, M. G., Tyndall, G. S., Orlando, J. J. and Brasseur, G. P.: A global simulation of tropospheric ozone and related tracers: Description and evaluation of MOZART, version 2, J. Geophys. Res. Atmos., 108(D24), n/a-n/a, doi:10.1029/2002JD002853, 2003.

Jacob, D. J. and Winner, D. a.: Effect of climate change on air quality, Atmos. Environ., 43(1), 51–63, doi:10.1016/j.atmosenv.2008.09.051, 2009.

Kim, M. J., Park, R. J., Ho, C.-H., Woo, J.-H., Choi, K.-C., Song, C.-K. and Lee, J.-B.: Future ozone and oxidants change under the RCP scenarios, Atmos. Environ., 101, 103–115, doi:10.1016/J.ATMOSENV.2014.11.016, 2015.

Langner, J., Engardt, M., Baklanov, A., Christensen, J. H., Gauss, M., Geels, C., Hedegaard, G. B., Nuterman, R., Simpson, D., Soares, J., Sofiev, M., Wind, P. and Zakey, A.: A multi-model study of impacts of climate change on surface ozone in Europe, Atmos. Chem. Phys., 12(21), 10423–10440, doi:10.5194/acp-12-10423-2012, 2012.

Lapina, K., Henze, D. K., Milford, J. B., Cuvelier, C. and Seltzer, M.: Implications of RCP emissions for future changes in vegetative exposure to ozone in the western U.S., Geophys. Res. Lett., 42(10), 4190–4198, doi:10.1002/2015GL063529, 2015.

Liao, H., Chen, W.-T. and Seinfeld, J. H.: Role of climate change in global predictions of future tropospheric ozone and aerosols, J. Geophys. Res., 111(D12), D12304, doi:10.1029/2005JD006852, 2006.

Lin, S.-J., Rood, R. B., Lin, S.-J. and Rood, R. B.: Multidimensional Flux-Form Semi-Lagrangian Transport Schemes, Mon. Weather Rev., 124(9), 2046–2070, doi:10.1175/1520-0493(1996)124<2046:MFFSLT>2.0.CO;2, 1996.

Meinshausen, M., Smith, S. J., Calvin, K., Daniel, J. S., Kainuma, M. L. T., Lamarque, J.-F., Matsumoto, K., Montzka, S. A., Raper, S. C. B., Riahi, K., Thomson, A., Velders, G. J. M. and Vuuren, D. P. P.: The RCP greenhouse gas concentrations and their extensions from 1765 to 2300, Clim. Change, 109(1–2), 213–241, doi:10.1007/s10584-011-0156-z, 2011.

Pfister, G. G., Walters, S., Lamarque, J.-F., Fast, J., Barth, M. C., Wong, J., Done, J., Holland, G. and Bruyère, C. L.: Projections of future summertime ozone over the U.S, , doi:10.1002/2013JD020932, n.d.

Pommier, M., Fagerli, H., Gauss, M., Simpson, D., Sharma, S., Sinha, V., Ghude, S. D., Landgren, O., Nyiri, A. and Wind, P.: Impact of regional climate change and future emission scenarios on surface O&lt;sub&gt;3&lt;/sub&gt; and PM&lt;sub&gt;2.5&lt;/sub&gt; over India, Atmos. Chem. Phys., 18(1), 103–127, doi:10.5194/acp-18-103-2018, 2018.

Putman, W. M. and Lin, S.-J.: Finite-volume transport on various cubed-sphere grids, J. Comput. Phys., 227(1), 55–78, doi:10.1016/j.jcp.2007.07.022, 2007.

Racherla, P. N. and Adams, P. J.: Sensitivity of global tropospheric ozone and fine particulate matter concentrations to climate change, J. Geophys. Res., 111(D24), D24103, doi:10.1029/2005JD006939, 2006.

Racherla, P. N. and Adams, P. J.: U.S. Ozone Air Quality under Changing Climate and Anthropogenic Emissions, Environ. Sci. Technol., 43(3), 571–577, doi:10.1021/es800854f, 2009.

Rasmussen, D. J., Fiore, A. M., Naik, V., Horowitz, L. W., McGinnis, S. J. and Schultz, M. G.: Surface ozone-temperature relationships in the eastern US: A monthly climatology for evaluating chemistry-climate models, Atmos. Environ., 47, 142–153, doi:10.1016/J.ATMOSENV.2011.11.021, 2012.

Rieder, H. E., Fiore, A. M., Horowitz, L. W. and Naik, V.: Projecting policy-relevant metrics for high summertime ozone pollution events over the eastern United States due to climate and emission changes during the 21st century, J. Geophys. Res. Atmos., 120(2), 784–800, doi:10.1002/2014JD022303, 2015.

Rohde, R. A. and Muller, R. A.: Air Pollution in China: Mapping of Concentrations and Sources, edited by A. Ding, PLoS One, 10(8), e0135749, doi:10.1371/journal.pone.0135749, 2015.

Stevenson, D. S., Dentener, F. J., Schultz, M. G., Ellingsen, K., van Noije, T. P. C., Wild, O., Zeng, G., Amann, M., Atherton, C. S., Bell, N., Bergmann, D. J., Bey, I., Butler, T., Cofala, J., Collins, W. J., Derwent, R. G., Doherty, R. M., Drevet, J., Eskes, H. J., Fiore, A. M., Gauss, M., Hauglustaine, D. A., Horowitz, L. W., Isaksen, I. S. A., Krol, M. C., Lamarque, J.-F., Lawrence, M. G., Montanaro, V., Müller, J.-F., Pitari, G., Prather, M. J., Pyle, J. A., Rast, S., Rodriguez, J. M., Sanderson, M. G., Savage, N. H.,

Shindell, D. T., Strahan, S. E., Sudo, K. and Szopa, S.: Multimodel ensemble simulations of present-day and near-future tropospheric ozone, J. Geophys. Res., 111(D8), D08301, doi:10.1029/2005JD006338, 2006.

Stevenson, D. S., Young, P. J., Naik, V., Lamarque, J.-F., Shindell, D. T., Voulgarakis, A., Skeie, R. B., Dalsoren, S. B., Myhre, G., Berntsen, T. K., Folberth, G. A., Rumbold, S. T., Collins, W. J., MacKenzie, I. A., Doherty, R. M., Zeng, G., van Noije, T. P. C., Strunk, A., Bergmann, D., Cameron-Smith, P., Plummer, D. A., Strode, S. A., Horowitz, L., Lee, Y. H., Szopa, S., Sudo, K., Nagashima, T., Josse, B., Cionni, I., Righi, M., Eyring, V., Conley, A., Bowman, K. W., Wild, O. and Archibald, A.: Tropospheric ozone changes, radiative forcing and attribution to emissions in the Atmospheric Chemistry and Climate Model Intercomparison Project (ACCMIP), Atmos. Chem. Phys., 13(6), 3063–3085, doi:10.5194/acp-13-3063-2013, 2013.

Stohl, A., Aamaas, B., Amann, M., Baker, L. H., Bellouin, N., Berntsen, T. K., Boucher, O., Cherian, R., Collins, W., Daskalakis, N., Dusinska, M., Eckhardt, S., Fuglestvedt, J. S., Harju, M., Heyes, C., Hodnebrog, Ø., Hao, J., Im, U., Kanakidou, M., Klimont, Z., Kupiainen, K., Law, K. S., Lund, M. T., Maas, R., MacIntosh, C. R., Myhre, G., Myriokefalitakis, S., Olivié, D., Quaas, J., Quennehen, B., Raut, J.-C., Rumbold, S. T., Samset, B. H., Schulz, M., Seland, Ø., Shine, K. P., Skeie, R. B., Wang, S., Yttri, K. E. and Zhu, T.: Evaluating the climate and air quality impacts of short-lived pollutants, Atmos. Chem. Phys., 15(18), 10529–10566, doi:10.5194/acp-15-10529-2015, 2015.

Szopa, S., Balkanski, Y., Schulz, M., Bekki, S., Cugnet, D., Fortems-Cheiney, A., Turquety, S., Cozic, A., Déandreis, C., Hauglustaine, D., Idelkadi, A., Lathière, J., Lefevre, F., Marchand, M., Vuolo, R., Yan, N. and Dufresne, J.-L.: Aerosol and ozone changes as forcing for climate evolution between 1850 and 2100, Clim. Dyn., 40(9–10), 2223–2250, doi:10.1007/s00382-012-1408-y, 2013.

Tagaris, E., Manomaiphiboon, K., Liao, K.-J., Leung, L. R., Woo, J.-H., He, S., Amar, P. and Russell, A. G.: Impacts of global climate change and emissions on regional ozone and fine particulate matter concentrations over the United States, J. Geophys. Res., 112(D14), D14312, doi:10.1029/2006JD008262, 2007.

Wu, S., Mickley, L. J., Jacob, D. J., Rind, D. and Streets, D. G.: Effects of 2000–2050 changes in climate and emissions on global tropospheric ozone and the policy-relevant background surface ozone in the United States, J. Geophys. Res., 113(D18), D18312, doi:10.1029/2007JD009639, 2008a.

Wu, S., Mickley, L. J., Leibensperger, E. M., Jacob, D. J., Rind, D. and Streets, D. G.: Effects of 2000–2050 global change on ozone air quality in the United States, J. Geophys. Res., 113(D6), D06302, doi:10.1029/2007JD008917, 2008b.

Young, P. J., Archibald, A. T., Bowman, K. W., Lamarque, J.-F., Naik, V., Stevenson, D. S., Tilmes, S., Voulgarakis, A., Wild, O., Bergmann, D., Cameron-Smith, P., Cionni, I., Collins, W. J., Dalsøren, S. B., Doherty, R. M., Eyring, V., Faluvegi, G., Horowitz, L. W., Josse, B., Lee, Y. H., MacKenzie, I. A., Nagashima, T., Plummer, D. A., Righi, M., Rumbold, S. T., Skeie, R. B., Shindell, D. T., Strode, S. A., Sudo, K., Szopa, S. and Zeng, G.: Pre-industrial to end 21st century projections of tropospheric ozone from the Atmospheric Chemistry and Climate Model Intercomparison Project (ACCMIP), Atmos. Chem. Phys., 13(4), 2063–2090, doi:10.5194/acp-13-2063-2013, 2013.

Zhang, Y.-L. and Cao, F.: Fine particulate matter (PM2.5) in China at a city level, Sci. Rep., 5(1), 14884, doi:10.1038/srep14884, 2015.

Zhu, J. and Liao, H.: Future ozone air quality and radiative forcing over China owing to future changes in emissions under the Representative Concentration Pathways (RCPs), J. Geophys. Res. Atmos., 121(4), 1978–2001, doi:10.1002/2015JD023926, 2016.